Carbon Neutrality

REVIEW

Open Access

PEM water electrolysis for hydrogen production: fundamentals, advances, and prospects

Tongzhou Wang[1,2], Xuejie Cao[1,2] and Lifang Jiao[1,2*]

Abstract

Hydrogen, as a clean energy carrier, is of great potential to be an alternative fuel in the future. Proton exchange membrane (PEM) water electrolysis is hailed as the most desired technology for high purity hydrogen production and self-consistent with volatility of renewable energies, has ignited much attention in the past decades based on the high current density, greater energy efficiency, small mass-volume characteristic, easy handling and maintenance. To date, substantial efforts have been devoted to the development of advanced electrocatalysts to improve electrolytic efficiency and reduce the cost of PEM electrolyser. In this review, we firstly compare the alkaline water electrolysis (AWE), solid oxide electrolysis (SOE), and PEM water electrolysis and highlight the advantages of PEM water electrolysis. Furthermore, we summarize the recent progress in PEM water electrolysis including hydrogen evolution reaction (HER) and oxygen evolution reaction (OER) electrocatalysts in the acidic electrolyte. We also introduce other PEM cell components (including membrane electrode assembly, current collector, and bipolar plate). Finally, the current challenges and an outlook for the future development of PEM water electrolysis technology for application in future hydrogen production are provided.

Keywords: PEM water electrolysis, Hydrogen production, hydrogen evolution reaction, Oxygen evolution reaction

1 Introduction

Carbon neutrality means having net-zero carbon dioxide emissions. Current issues on climate change and global warming have been an ongoing concern for the world, environmental issues will strongly affect us if we do not start taking them seriously [1–3]. In order to reduce carbon emissions and achieve carbon neutrality, it is an urgency to develop clean and sustainable fuels from renewable energy resources such as wind and solar power, geothermal, and biomass energy to replace traditional fossil fuels. In this respect, hydrogen fuel, with high gravimetric energy density (140 MJ kg^{-1}) and only generates water as a byproduct without any environmental concern, has been hailed as the unrivaled clean energy carrier to reduce conventional fossil fuels consumption and relieve aggravating environmental problems [4, 5]. Currently, hydrogen is mainly produced through steam reforming of fossil fuels under harsh conditions, which are restrained by the complex operation and emission of carbon dioxide. Electrochemical water splitting is an effective and clean method to produce high-purity hydrogen by using renewable energy, which has ignited new interests in the past decades. During the water electrolysis process, hydrogen evolution reaction (HER) occurs at the cathode and oxygen evolution reaction (OER) operates at the anode [6–8]. Theoretically, it only needs the voltage of 1.23 V to drive the water electrolysers to obtain hydrogen production. However, it usually needs a much larger voltage of 1.8–2.0 V in the practical electrolysis

*Correspondence: jiaolf@nankai.edu.cn

[1] Key Laboratory of Advanced Energy Materials Chemistry (Ministry of Education), Renewable Energy Conversion and Storage Center (RECAST), College of Chemistry, Nankai University, Tianjin 300071, China
Full list of author information is available at the end of the article

process, due to the overpotentials on both cathode and anode. Therefore, various kinds of electrocatalysts have been developed to reduce the overpotentials for both HER and OER [9–11].

Electrochemical water electrolysis can be classified into three main types based on the type of electrolytes and operating conditions: alkaline water electrolysis (AWE), solid oxide electrolysis (SOE), and proton exchange membrane (PEM) water electrolysis, as shown in Fig. 1. AWE operates at the high concentrations of alkaline solutions and employs diaphragm (such as asbestos, polyethersulfone (PES), microporous polymer membrane, glass reinforced polyphenylene sulfide (PPS) compounds et al.) to separate the produced gases from the cathode and anode, which suffers from low operating pressure, sluggish anion transport kinetics and limited current density. SOE operates at high pressure and high temperature of 500–850°C, but is plagued by unsatisfactory catalyst durability and membrane degradation. PEM electrolysis is considered a splendid method for high-purity hydrogen production in the future industrial application, due to its high current density, greater energy efficiency, smaller gas crossover, wider operating temperatures (20–80°C) [12], smaller mass-volume characteristic, more importantly, the specialty of adaptive to renewable energy volatility. In the past decades, significant progress has been made in PEM electrolysis technology. For example, a high cell electrolysis efficiency of 94.4% and a very low cell voltage of 1.567 V were obtained by Marshall [13] to reach the current density of 1 A cm^{-2}. A stable voltage for over 5000 h during 2 A cm^{-2} and a peak operating current density of 20 A cm^{-2} has been acquired [14]. Despite the many advantages and bright prospects of PEM electrolysers, the practical industrial application of this technology is plagued by the prohibitively exorbitant cost and extreme degradation of electrocatalysts under an acidic environment, especially for OER catalysts that simultaneously experience the acidic and strongly oxidative environments. To address these problems, great research efforts have been directed towards reducing the usage of noble metals and exploiting noble-metal-free catalysts, improving the intrinsic catalytic performance and the durability of catalysts in the acidic electrolyte. To date, the materials for acidic HER are mainly Pt-based material, transition metal dichalcogenides (TMDs), and transition metal phosphides (TMPs). The most popular acidic OER electrocatalysts are focused on precious Ir and Ru-based materials, perovskites, and nonprecious metal oxides. At present, the electrocatalytic performance and stability for both HER and OER have made significant progress, stimulating the development of PEM water electrolysis.

Here, we provide recent progress of the PEM water electrolysis for hydrogen production. In this review, we first compare the distinction between AEW, SOE, and PEM to emphasize the advantages of PEM water electrolysers in producing hydrogen. Then, we focus on the recent development of acidic HER electrocatalysts and OER electrocatalysts for PEM water electrolysis. Then, we introduce other key materials for PEM water electrolysis, such as membrane electrode assembly (MEA), current collector, and bipolar plate. Finally, we propose the current challenges and perspectives on the development of PEM water electrolysis technology for application in future hydrogen production.

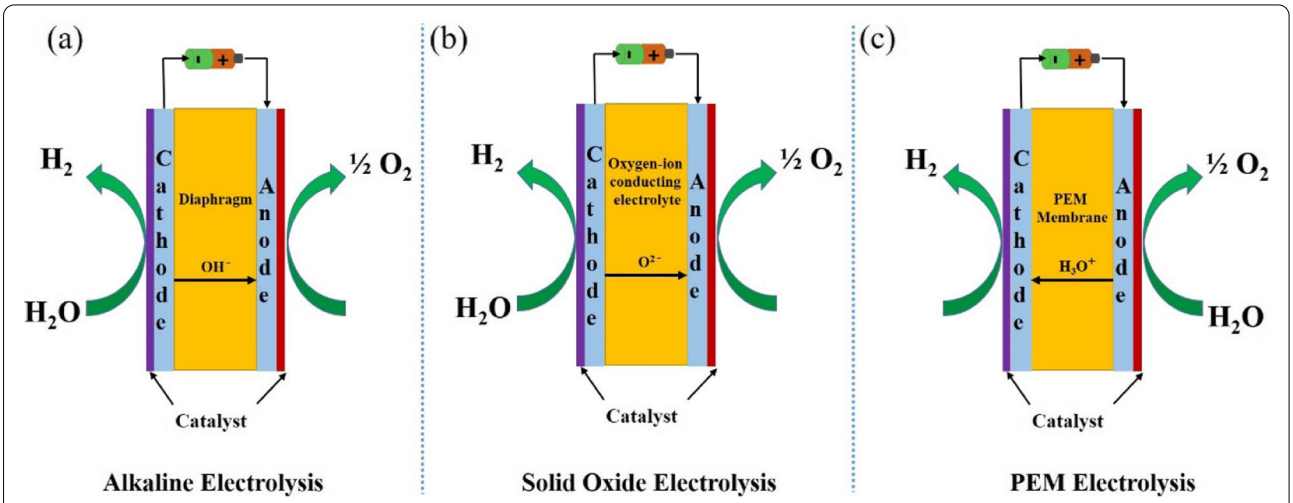

Fig. 1 Schematic illustration of (**a**) alkaline water electrolysis, (**b**) solid oxide electrolysis, and (**c**) proton exchange membrane water electrolysis

2 Water electrolysis technologies

2.1 Alkaline water electrolysis (AWE)

AWE is a well-established technology for hydrogen production and this phenomenon was first found by Troostwijk and Diemann in 1789 [12]. AWE usually operates at lower temperatures between 30–90°C and uses alkaline KOH/NaOH aqueous solution with a typical concentration of 20–30% as the electrolyte. In alkaline electrolysers, the diaphragm and porous nickel-based materials are usually used as asbestos and electrode. Alkaline electrolysis is a mature process, which only needs low investment and operation costs. However, the AWE usually exhibits a low operating current density of 200–400 mA cm^{-2} and an energy efficiency of approximately 62–82% [15]. Moreover, the pressure between the anode and cathode sides needs to keep balanced, avoiding the hydrogen or oxygen generated by the electrolysis penetrating the diaphragm to the other side and resulting in the explosion risk.

2.2 Solid oxide electrolysis (SOE)

SOE has received an enormous amount of attention because of its high efficiency and environmental friendliness, the needed electrical power could be provided by sustainable energy sources [16]. However, SOE works at high temperatures (500–850°C) and pressure, water is in the form of steam during the SOE process. The most commonly used electrolyte material is yttria-stabilized zirconia, the conventional high-temperature oxygen-ion conductor. However, the high temperatures result in the fast deterioration of catalytic performance, and achieving the long-term operation of SOE is a challenge. Meanwhile, the produced hydrogen can form a mixture with steam and needs an additional procedure to acquire high purity hydrogen.

2.3 Proton exchange membrane water electrolysis (PEM)

PEM electrolysis has been known for over sixty years and was developed by General Electric, where a solid sulfonated polystyrene membrane is used as the electrolyte. This technology is also named polymer electrolyte membrane electrolysis. The proton exchange membrane acts as both the gas separator and the electrolyte. In the electrolysis process, only deionized water is injected into the cell without any electrolytic additives. There are a variety of advantages of PEM electrolysis, such as high current density, greater energy efficiency, low gas permeability, wider operating temperatures (20–80°C) [12], easy handling and maintenance. However, the popular electrocatalysts for PEM electrolysis are precious metals (Pt, Ir, Ru), the exorbitant cost of these precious metal makes PEM electrolysis a relatively higher investment than alkaline electrolysis. In this regard, researchers have paid tremendous efforts for reducing the cost and improving the intrinsic activity of PEM electrocatalysts. As shown in Table 1, listing the typical characteristics of three water electrolysis technologies.

3 Electrocatalysts for PEM water electrolysis

3.1 Electrocatalysts for hydrogen evolution reaction (HER)

The predicament for HER in PEM electrolysis is the development of high-activity and stability catalysts for the cathode. Presently, platinum (Pt) and Pt-based materials are recognized as the state-of-the-art electrocatalysts for the cathode side in PEM electrolysers [17, 18], which exhibit decent electrochemical activity for the HER in acidic electrolytes. However, the large-scale

Table 1 Typical characteristics of three water electrolysis technologies

Water electrolysis technologies	Alkaline water electrolysis (AWE)	Proton exchange membrane water electrolysis (PEM)	Solid oxide electrolysis (SOE)
Electrode reactions	Cathode: $4H_2O + 4e^- \rightarrow 4OH^- + 2H_2$ Anode: $4OH^- \rightarrow 2H_2O + O_2 + 4e^-$	Cathode: $4H^+ + 4e^- \rightarrow 2H_2$ Anode: $2H_2O \rightarrow 4H^+ + 4e^- + O_2$	Cathode: $2H_2O + 4e^- \rightarrow 2O^{2-} + 2H_2$ Anode: $2O^{2-} \rightarrow 4e^- + O_2$
Current density (A/cm^2)	0.2 – 0.4	1 – 3	0.3 – 0.5
Efficiency (%)	62 – 82	67 – 82	81 – 92
Operating temperature (°C)	≤ 90	≤ 80	~800
Electrolysis energy consumption (kWh/Nm^3)	4.5 – 5.5	4.0 – 5.0	< 3.5
Response time	minutes	seconds	–-
Electrolyser life (h)	60,000	80,000	< 20,000
Applicability	wide range of commercial application	commercial application	laboratory scale
Disadvantages and challenges	corrosive electrolyte, gas permeation, slow dynamics	high cost of catalyst and proton exchange membrane	mechanically unstable electrodes, safety issues

deployment of these catalysts is constrained by the high cost and limited reserves. For this, considerable efforts have been devoted to exploring various methods to reduce Pt mass loading and exploit other Pt-free electrocatalysts [19–27]. Lim and co-workers [28] prepared a Pt@N-containing carbon core–shell catalyst on carbon nanofibers (Pt@CS/CNF), which exhibited excellent catalytic activity and durability. They found that the graphitic N and pyridinic N on the carbon shell could not only offer additional catalytic active sites for HER, but also impede the active Pt core from dissolution and agglomeration, improving the stability (Fig. 2a-d). Zhong and co-workers [21] adopted an ultralow-temperature solution method to prepare a single atom Pt anchored on carbon nanotubes (SA-Pt-CNTs), which reduced Pt usage and improved the intrinsic HER activity in acidic media, a low overpotential of only 41 mV to achieve the current density of 10 mA cm^{-2}. The aberration-corrected high-angle annular dark-field scanning transmission electron microscopy (HAADF-STEM) demonstrates Pt atoms were atomically dispersed. Density functional theory (DFT) demonstrated the high electrocatalytic activity is attributed to the interaction between CNTs and Pt atoms, which leads to the downshift of the d-band center and facilitates the H desorption (Fig. 2e-g). Xu et al. [22] rationally designed atomically dispersed Pt anchored on amorphous MoO_x (Pt-SA/α-MoO_x), which unfolded a low overpotential of 19 mV at 10 mA cm^{-2} and excellent mass activity of 52.0 A mg_{Pt}^{-1} at the overpotential of 50 mV in 0.5 M H_2SO_4. Additionally, it also exhibited a low Tafel slope of 123 mV dec^{-1} and long-time durability. DFT results revealed that the remarkable performance is attributed to the synergistic effect between unsaturated Pt atoms and amorphous MoO_x, which are beneficial for atomic hydrogen adsorption. Xia and co-workers [29] reported a series of carbon-supported ultrasmall high-entropy alloy nanoparticles (us-HEA NPs) through a general and ultrafast chemical co-reduction method. In 0.5 M H_2SO_4 electrolyte, this us-HEA NPs exhibited an eminent mass activity of 28.3 A mg^{-1} at -0.05 V, which shows a promising prospect for HER in PEM electrolysis.

In recent years, various transition metal dichalcogenides have been developed as acidic HER electrocatalysts [30], such as MoS_2 [31–35], WS_2 [36], $MoSe_2$ [37–39], and WSe_2 [40], which have shown to be splendid cathodic materials for HER. Nørskov and co-workers [25] investigated the HER performance of MoS_2 and fabricated an MEA based on a Nafion proton exchange membrane, which showed a lower current density of 10 mA cm^{-2} at the overpotential of 175 mV. Kim et al. [41] reported a simple one-step electrodeposition method to prepare amorphous molybdenum sulfide (MoS_x) on carbon paper and used as the gas-diffusion layer for PEM water electrolysis, which displayed acceptable cell performance. Because sulfur atoms on the catalyst surface with different binding energy values, they could extremely affect the

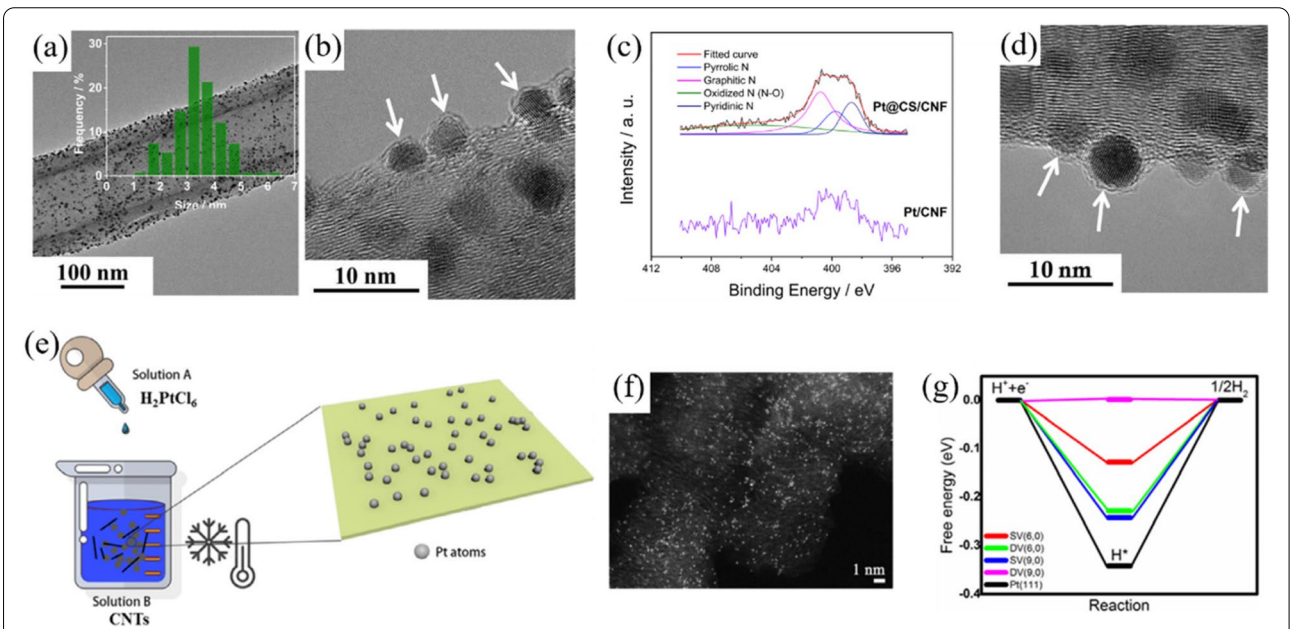

Fig. 2 **a**,**b** TEM images and (**c**) N 1 s XPS spectra of Pt@CS/CNF. **d** TEM images of Pt@CS/CNF after durability test [28]. **e** A scheme showing the synthesis of Pt-CNTs through ultralow-temperature solution reduction. **f** HAADF-STEM image of Pt-CNTs. **g** Calculated ΔG_{H^*} on different sites for HER [21]

intrinsic activity of MoS_x and facilitate the HER performance. The 1T phase of TMDs possesses high electrical conductivity and a larger number of active sites compared to the 2H phase [42–44], which could result in a higher charger transfer rate in the electrochemical process. Recently, Kang and co-workers [45] successfully synthesized $Mo_{1-x}V_xSe_2$ alloy nanosheets through a colloidal reaction, which could lead to the phase transition from a semiconducting 2H phase $MoSe_2$ to the metallic 1T phase VSe_2 (Fig. 3). DFT calculations suggested the decent electrocatalytic activity attributed to the V and Se vacancies, which are beneficial for the phase transition from the 2H phase to the 1T phase and forming the intermediates in HER. Additionally, various cation-doping is also an effective strategy to tune the surface electronic structure of catalysts and optimize the hydrogen adsorption free energy, improving the electrocatalytic HER activity [46, 47]. Morozan et al. [24] adopted microwave irradiation or heat treatment in a furnace under inert and reductive atmospheres to prepare the bimetallic FeMoS catalyst, which presented a low overpotential of 140 mV at the current density of 10 mA cm^{-2}. Combining with

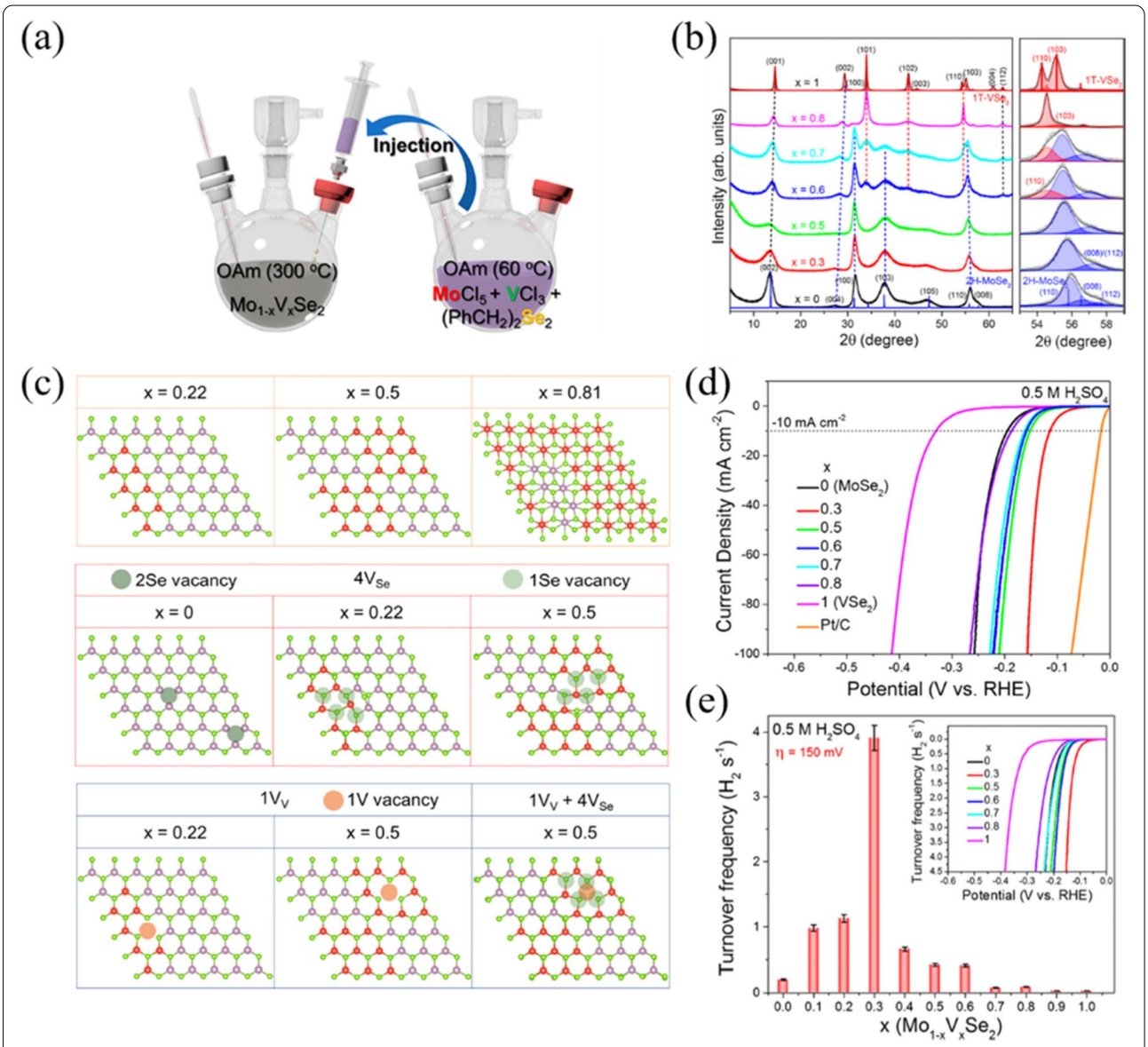

Fig. 3 **a** Schematic illustration of the precursor of $Mo_{1-x}V_xSe_2$ synthesis. **b** XRD patterns of $Mo_{1-x}V_xSe_2$ nanosheets with different Mo and V molar ratios. **c** Ball-and-stick model of $Mo_{1-x}V_xSe_2$ with different vacancies. **d** OER polarization curves and (**e**) Turnover frequency curves of $Mo_{1-x}V_xSe_2$ and Pt/C catalysts [45]

carbon nanotubes (CNTs), the composite catalyst could operate at 500 mA cm^{-2} using a voltage of less than 300 mV compared to using Pt as the cathode catalyst in PEM electrolyser. Zhao et al. [48] prepared an ultrastable Pd-doped MoS_2 material and supported on a vertical graphene network (VGN@Pd-MoS_2), which exhibited a stable operation over 1000 h at 10 mA cm^{-2} and provide a prospect to replace Pt for PEM electrolysis.

Apart from Pt and TMDs, researchers also devoted to developing various alternative electrocatalysts for the hydrogen evolution reaction in acidic electrolytes [26, 27, 49–51]. Li and co-workers [26] proposed a universal strategy to prepare a series of Ni-activated transition metal carbides (TMCs) on Ni foam coated with graphene (Ni-GF) and further optimize the HER activity of these TMCs. After the introduction of Ni atoms, these Ni-GF/TMCs exhibited much reduced overpotentials and intriguing durability toward HER, as displayed in Fig. 4a-c. They found that the superior HER performance hinges on the unique structural characteristics and optimized electronic synergy of Ni-activated TMCs. The doping of Ni atoms on the surface of TMCs could effectively regulate the d-electron structure, which can not only significantly enhance the exposed active sites, but also improve the intrinsic catalytic activity (Fig. 4d, e). Additionally, the high specific surface areas and unique 3D skeleton structure could facilitate a fast electron transfer rate and efficient release of hydrogen bubbles. Sapountzi et al. [50] prepared highly crystalline FeP NPs with predominantly exposed [010] facets on a conductive carbon support and presented high activity in HER. They also assembled a full-cell PEM water electrolysis by using FeP as cathode and a commercial $IrRuO_x$ as anode, which could reach a current density of 0.2 A cm^{-2} at a voltage of 2.06 V and operate steadily for up to 36 h continuously. Ito and co-workers [27] further improved the acid stablility through graphene-covering approach and investigated the effect of graphene-covering layers on HER activities of Ni and Cu. They found that the graphene could optimize the HER activity and impede the corrosion, and the ability of protons to penetrate graphene manipulates the HER performance of these graphene-covered non-noble metals.

3.2 Electrocatalysts for oxygen evolution reaction (OER)

Because of the pivotal role of OER in water electrolysis, the energy community has put substantial efforts into exploiting admirable OER catalysts. Due to the acidic and strongly oxidative environments, developing high-active and robust electrocatalysts for OER in PEM electrolysers is an arduous challenge. To date, Ir-based and Ru-based catalysts are the most popular OER electrocatalysts in acid. Ru-based catalysts exhibit super OER activity but unsatisfactory stability compared with Ir-based catalysts. In this section, we systematically summarize the reports about Ir-based and Ru-based catalysts in the past decades (Table 2).

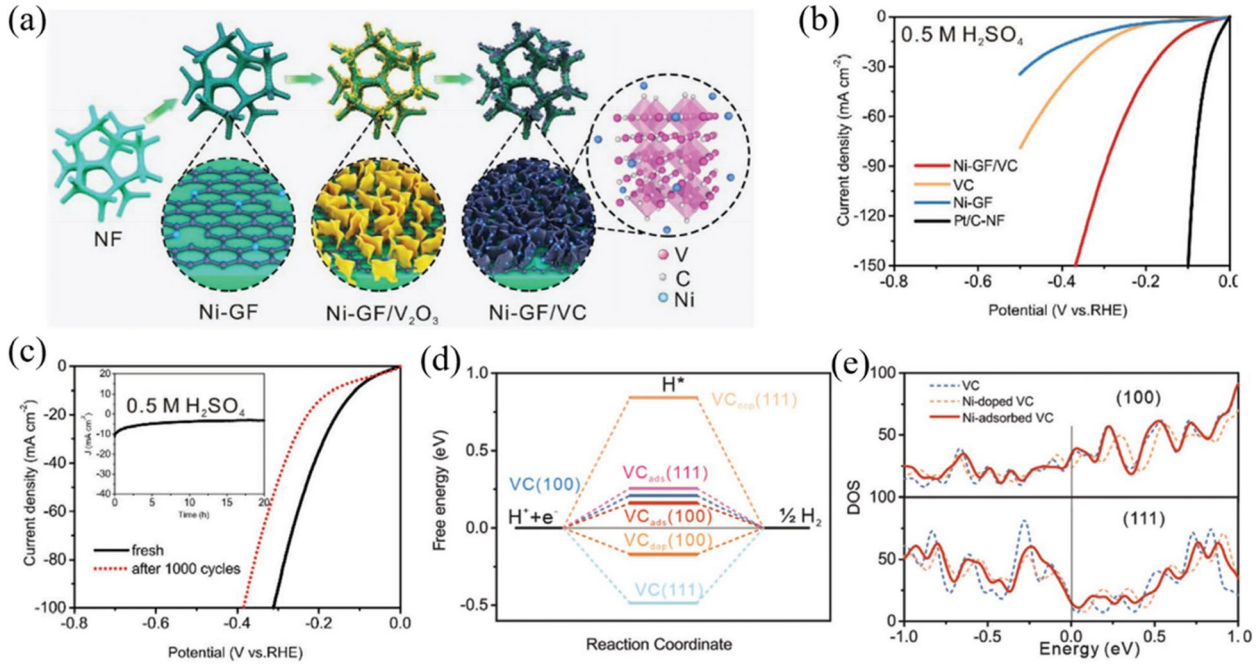

Fig. 4 **a** Schematic illustration of the synthesis of Ni-GF/TMC catalyst. **b** HER performance and (**c**) stability of Ni-GF/TMCs catalysts. **d** Calculated ΔG_{H^*} for HER. **e** the total DOS patterns of different catalysts [26]

Table 2 Comparison of acidic OER performance with different catalysts

Catalyst	Substrate	Electrolyte	Stability	Loading	η_{10} (mV)	Tafel slope (mV dec^{-1})	Ref
Ultrafine Ir NPs	GC	0.5 M $HClO_4$	1000 cycles or 20,000 s@10 mA cm^{-2}	90 μg_{Ir} cm^{-2}	290	65.1	[52]
Ir@HEDP/CNBs	GC	0.1 M $HClO_4$	5 h@10 mA cm^{-2}	-	290	49.1	[53]
Ir-SA@Fe@NCNT	GC	0.5 M H_2SO_4	12 h@10 mA cm^{-2}	1.14 μg_{Ir} cm^{-2}	250	58.2	[54]
$Ir_{0.06}Co_{2.94}O_4$	Au electrode	0.1 M $HClO_4$	200 h@10 mA cm^{-2}	5 μg_{Ir} cm^{-2}	292	45	[55]
3D Ir	GC	0.1 M $HClO_4$	8 h@2.5 mA cm^{-2}	11.5 μg_{Ir} cm^{-2}	240	40.8	[56]
Ir/g-C_3N_4/NG	GC	0.5 M H_2SO_4	2000 cycles	6.7 μg_{Ir} cm^{-2}	287	72.8	[57]
Mesoporous Ir nanosheets	GC	0.5 M H_2SO_4	8 h@10 mA cm^{-2}	-	240	49	[58]
Amorphous Ir nanosheets	GC	0.1 M $HClO_4$	5000 cycles	0.2 mg cm^{-2}	255	40	[59]
Ru–N-C	GC	0.5 M H_2SO_4	30 h@1.49 V	0.28 mg cm^{-2}	267	52.6	[60]
Ru_1-Pt_3Cu	GC	0.1 M $HClO_4$	28 h@10 mA cm^{-2}	1.92 μg_{Ru} cm^{-2}	220	-	[61]
Ru/RuS_2	GC	0.5 M H_2SO_4	3000 cycles or 24 h@10 mA cm^{-2}	0.849 mg cm^{-2}	201	47.2	[62]
fcc-Ru octahedral	GC	0.05 M H_2SO_4	-	-	168	47.8	[63]
IrNi NPNWs	GC	0.1 M $HClO_4$	200 min@5 mA cm^{-2}	25 μg_{Ir} cm^{-2}	283	56.7	[64]
Ir_3Cu	GC	0.1 M $HClO_4$	12 h@5 mA cm^{-2}	-	298	47.4	[65]
IrNi NCs	GC	0.1 M $HClO_4$	2 h@5 mA cm^{-2}	12.5 μg_{Ir} cm^{-2}	280	-	[66]
$Rh_{22}Ir_{78}$	GC	0.5 M H_2SO_4	2000 cycles	9.8 μg_{Ir} cm^{-2}	292	101	[67]
IrRu@Te	GC	0.5 M H_2SO_4	20 h@10 mA cm^{-2}	0.6 mg cm^{-2}	220	35	[68]
Co-RuIr	Au electrode	0.1 M $HClO_4$	25 h@10 mA cm^{-2}	-	235	66.9	[69]
$Pt_{39}Ir_{10}Pd_{11}$	GC	0.1 M $HClO_4$	-	16.8 $\mu g_{Pt+Ir+Pd}$ cm^{-2}	372	128.7	[70]
IrNiCu DNF	GC	0.1 M $HClO_4$	2500 cycles	20 μg_{Ir} cm^{-2}	300	48	[71]
Co-IrCu	GC	0.1 M $HClO_4$	2000 cycles	20 μg_{Ir} cm^{-2}	290	50	[72]
IrCoNi PHNC	GC	0.1 M $HClO_4$	200 min@5 mA cm^{-2}	10 μg_{Ir} cm^{-2}	303	53.8	[73]
IrO_xQD/GDY	CC	0.5 M H_2SO_4	3000 cycles or 20 h@1.6 V	-	236	70	[74]
$IrHf_xO_y$	GC	0.1 M $HClO_4$	6 h@5 mA cm^{-2}	-	330	60	[75]
$Cr_{0.6}Ru_{0.4}O_2$	GC	0.5 M H_2SO_4	10 h@10 mA cm^{-2}	-	178	58	[76]
$W_{0.2}Er_{0.1}Ru_{0.7}O_{2-\delta}$	CP	0.5 M H_2SO_4	500 h@10 mA cm^{-2}	0.33 mg cm^{-2}	168	66.8	[77]
a/c-RuO_2	GC	0.1 M $HClO_4$	60 h@10 mA cm^{-2}	0.404 mg cm^{-2}	205	48.6	[78]
$RuIrO_x$	GC	0.5 M H_2SO_4	24 h@10 mA cm^{-2}	10 μg_{Ir+Ru} cm^{-2}	233	42	[79]

GC is glassy carbon, *CC* is carbon cloth, *CP* is carbon paper

Ir metal catalysts Ir metal is a vital electrocatalyst for OER under an acidic environment and has gained explosive interest because of its low overpotentials and unique stability. The catalytic performance is largely credited to the morphology, particle size, crystal structure, and substrate materials. As a result, various Ir-metal materials have been explored to optimize the OER activity and reduce the amount of precious metal.

Decreasing particle size or preparing ultrathin structure is an effective method to maximize surface area and expose more active sites [80], beneficial for improving the catalytic activity [81, 82]. Ultrafine monodisperse Ir NPs with narrow size distribution and high dispersion were successfully synthesized through a colloidal method [52]. Due to the ultrafine particle size and uniform dispersion, this catalyst exhibited startling catalytic performance for acidic OER and exceeded commercial IrO_2 catalyst. Carbon nanobowls supported ultrafine Ir nanocrystal (Ir@HEDP/CNBs) catalyst was prepared by Chen and co-workers [53], Fig. 5a-c show the ultrafine size and homogeneous distribution of Ir nanocrystal, as well as the high surface area and conductivity of CNBs, rendering it low OER overpotential of 290 mV at 10 mA cm^{-2} and excellent stability. Single atom catalysts (SACs) can realize the maximum atom utilization efficiency and reduce the amount of precious metal [83, 84]. In view of the severe activity decay of SACs in harsh acidic solutions, high-stable Ir SAC onto Fe NPs coated with nitrogen-doped carbon nanotubes (Ir-SA@Fe@NCNT) was prepared, which realized the ultralow Ir loading and superior OER performance with an overpotential of only 250 mV to reach 10 mA cm^{-2} in acidic solution. As shown in Fig. 5d-f, Qiao and co-workers [55] also reported a short-range ordered Ir SA integrated into Co oxide spinel structure and exhibited much higher acidic OER activity and excellent stability. A 3D Ir superstructure catalyst consisting of ultrathin Ir nanosheets to increase the accessible active

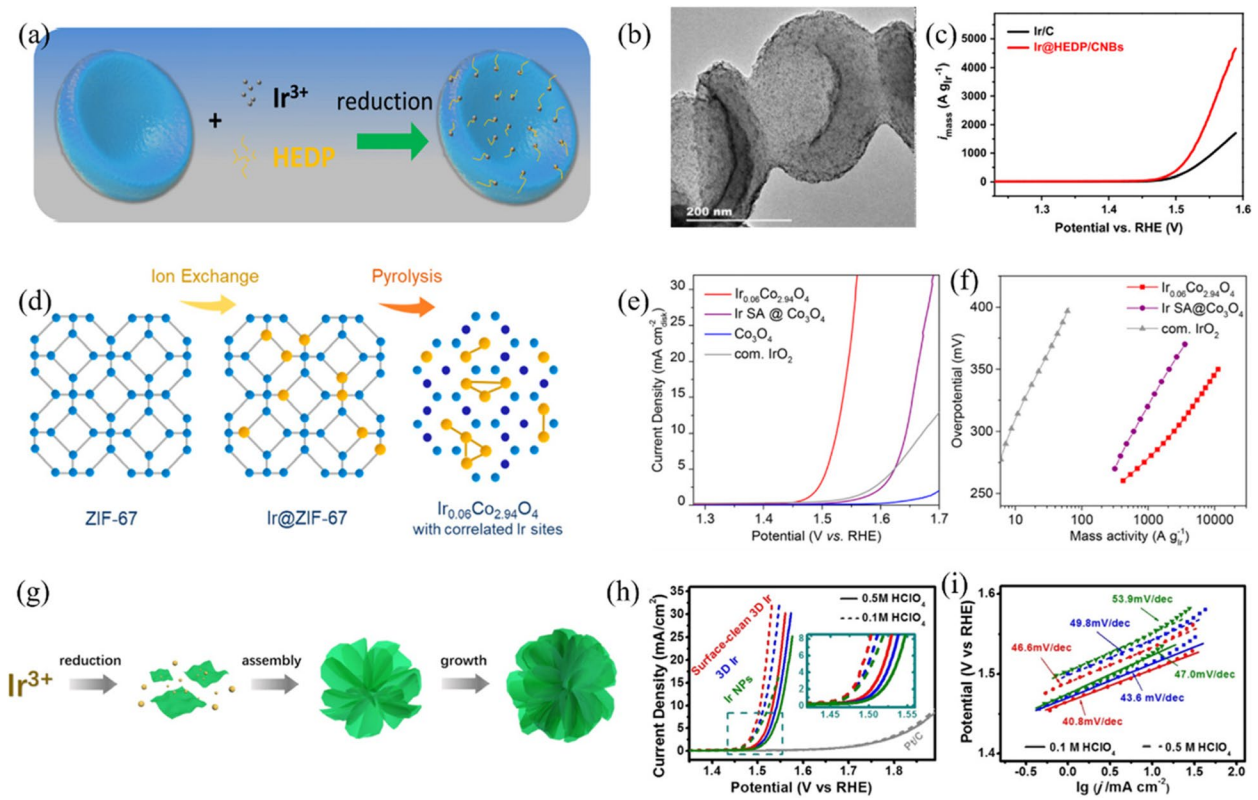

Fig. 5 **a** Synthesis and (**b**) TEM image of Ir@HEDP/CNBs. **c** OER performance of Ir@HEDP/CNBs and Ir/C in 0.1 M $HClO_4$ [53]. **d** Synthetic scheme of Ir SA catalyst. **e** LSV curves and (**f**) mass activity of various catalysts [55]. **g** Schematic illustration of synthesis 3D Ir superstructure. **h** OER performance and (**i**) Tafel slopes of 3D Ir superstructure, Ir NPs, and Pt/C catalysts in $HClO_4$ solution [56]

sites and active surface area was reported by Huang and co-workers [56]. This 3D Ir catalyst exhibited an unexpectedly low overpotential of 240 mV and intriguing durability with ignorable voltage degradation (Fig. 5g-i).

A robust and appropriate catalyst support is also important to improve activity and stability. Graphene, with decent electrical conductivity and chemical stability, high mechanical strength, and flexibility, has been used as a promising substrate material in diverse fields. Velasco-Vélez and co-workers [85] prepared electrochemically active Ir NPs on graphene and improved the acidic OER activity and stability. Shao and co-workers further adopted graphitic carbon nitride (g-C_3N_4) and nitrogen-doped graphene (NG) as a substrate to anchor monodispersed Ir NPs (Ir/g-C_3N_4/NG). This g-C_3N_4/NG substrate could effectively prevent the aggregation of Ir NPs and improve the reaction kinetics. The Ir/g-C_3N_4/NG catalyst can reach the current density of 10 mA cm^{-2} at a low overpotential of 287 mV, much superior to the pure Ir. Montmorillonite (MMT, $(Na,Ca)_{0.33}(Al,Mg)_2(Si_4O_{10})(OH)_2{\cdot}nH_2O$) is a natural mineral, which is easily available and cost-efficient. Boshnakova et al. [86] proved that MMT is a distinguished substrate to replace conventional carbon supports, the unique morphology and layered structure are conducive to enhancing the accessible active sites and improving the stability.

The preparation of catalysts with abundant porous structures or defects is an effective approach to expose more active surface area to the electrolyte environment and enhance the amount of the active sites. As shown in Fig. 6, Yamauchi and co-workers [58] reported an unprecedented type of 2D mesoporous Ir nanosheets through the formic acid assisted method, which served as both a reducing agent and a shape-directing agent. They found that the mesoporous structure was robust and this mesoporous Ir nanosheets also presented unrivaled electrocatalytic OER activity. This work opened a new dimension in the preparation of other porous 2D materials and further exploration of the paramount of porous structure on 2D materials for OER performance. Amorphous catalysts are often prepared due to their abundant active sites, inherent disordering, and an unsaturated coordination structure, which usually displayed more impressive catalytic performance than corresponding crystalline

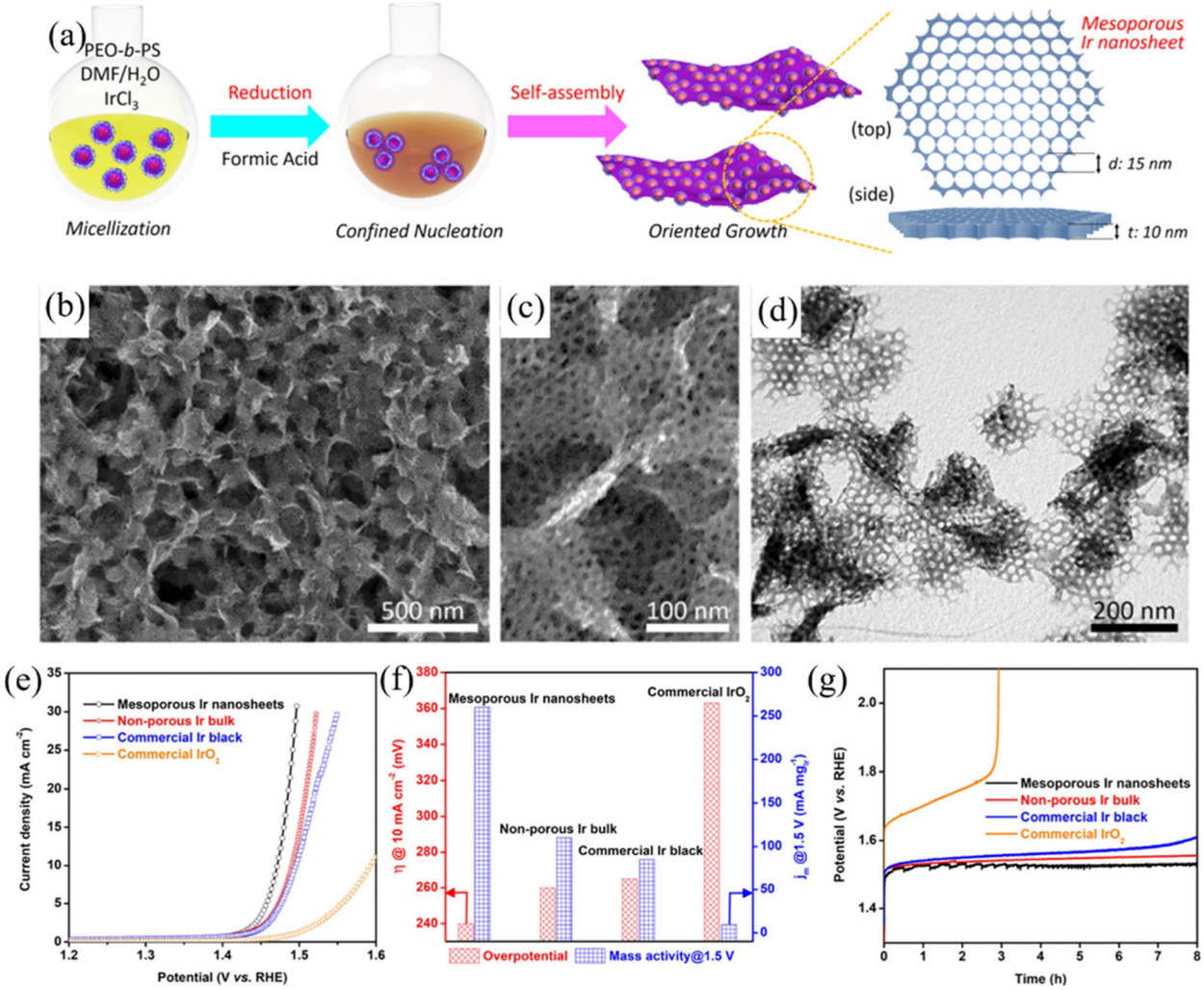

Fig. 6 **a** Formation mechanism of the mesoporous Ir nanosheets. **b**,**c** SEM and (**d**) TEM images of Ir nanosheets. **e**–**g** OER polarization curves, Ir mass activity and chronopotentiometry curves of catalysts [58]

materials [78, 87, 88]. Wu et al. [59] prepared a series of amorphous metal catalysts through a general and facile method. They found that the amorphous Ir nanosheets depicted intriguing acidic OER activity than crystalline Ir nanosheets and benchmark IrO_2 catalyst, which only required an overpotential of 255 mV to reach the current density of 10 mA cm^{-2} and exhibited robust durability with ignorable activity alleviation even after 5000 cycles in 0.1 M $HClO_4$ solution.

Ru metal catalysts Ruthenium (Ru) has been evaluated to be one of the promising active materials for acidic OER by virtue of its appropriate adsorption strength toward oxygenated intermediate species. Additionally, Ru is abundant in natural resources and cheaper than Ir metal. Unfortunately, the reported Ru-based catalysts are unstable, which is likely due to the oxidation of lattice oxygen and generation of oxygen vacancy, leading to the over-oxidation of Ru-based materials [61, 77]. To overcome this limit, great efforts have been dedicated to exploiting robust and efficient Ru-based electrocatalysts for OER in acid media [62, 89, 90].

Recently, Ru SACs have ignited much interest and exhibited extraordinary performance for acidic OER. It has demonstrated that the substrate and coordination environment have a significant effect on the electrocatalytic activity. As displayed in Fig. 7, a Ru SAC with the Ru_1-N_4 configuration anchored on nitrogen-carbon support displayed an exceptionally intrinsic activity, the mass activity could reach 3571 A g_{metal}^{-1} and a high turnover frequency of 3348 O_2 h^{-1}, as well as a low overpotential

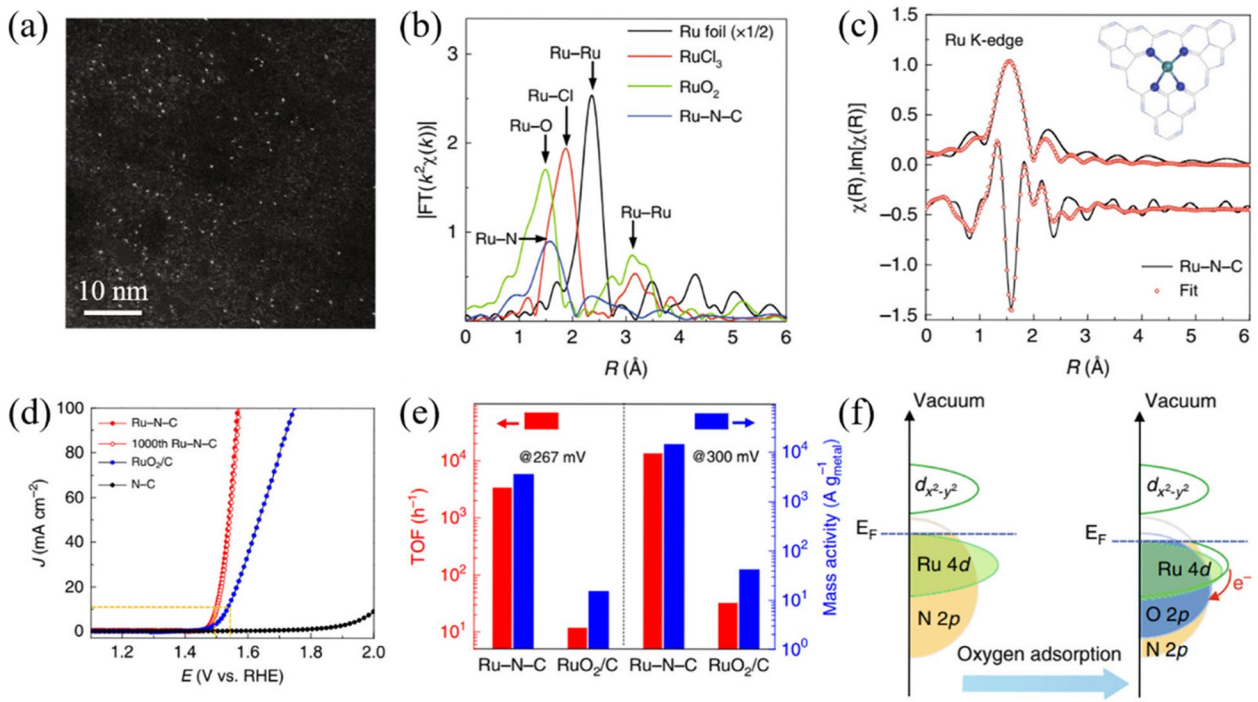

Fig. 7 **a** HAADF-STEM image of Ru SAC. **b** The Ru k-edge k^2-weighted Fourier transform spectra for Ru foil, $RuCl_3$, RuO_2, and Ru SAC. **c** R-space curve-fitting of ex-situ Ru–N-C. **d**,**e** OER performance of Ru SAC, RuO_2/C, and N–C catalysts. **f** The effect of oxygen adsorption on the electronic structure of Ru SAC [60]

[60]. Moreover, it also revealed decent stability and could operate steadily for 30 h in 0.5 M H_2SO_4 solution. Operando synchrotron radiation X-ray absorption fine structure (XAFS) spectroscopy and Fourier transform infrared (SR-FTIR) spectroscopy validated that adsorbed oxygen atom on Ru site to form O-Ru_1-N_4 site under the operating condition. The oxygen adsorption could downshift the Ru 4d band and increase the average valence state of Ru, which is responsible for reducing the limiting reaction barrier. Wu and co-workers [61] constructed a series of $PtCu_x$ alloys that supported Ru SACs through sequential acid etching and electrochemical leaching. Ru_1-Pt_3Cu as the best catalyst in this work, only need a low overpotential of 220 mV to reach a current density of 10 mA cm^{-2} and displayed ultra-long lifetime than benchmark RuO_2. From XPS and operando XAFS results, they demonstrated the valence state of Ru has no evident variation even after the stability test, preventing the over-oxidation of Ru. Further, they captured the OOH intermediate during the electrochemical process by using in-situ attenuated total reflection infrared (ATR-IR) spectroelectrochemical measurements, indicating the adsorbate evolution mechanism (AEM) instead of lattice oxygen evolution reaction (LOER) during the acidic OER reaction over Ru_1-Pt_3Cu. DFT calculations suggested that with the increase of Pt to Cu ratio, the compressive surface strain would lead to the upshift of the d-band center of Ru and enhancement of oxygen adsorption, resulting in the deteriorated performance.

Interface engineering is also an admirable approach to modulating the electronic environment, exposing abundant active sites, promoting electron transfer, and optimizing the electrocatalytic activity [91, 92]. Based on this, Mu and co-workers [62] prepared a laminar Ru/RuS_2 heterostructure catalyst through the synchronous reduction and sulfurization under the eutectic salt system for the first time. Theoretical calculation results suggested engineering of this heterostructure would endow it with higher electrical conductivity, charge redistribution over interfaces, and optimized adsorption strength of key intermediates, sequentially reducing the thermodynamic energy barriers.

The OER catalytic performance of Ru nanocrystals with different structures was investigated to explore the relationship between catalytic activity and crystal structures [63]. It is reported that the face-centered cubic (fcc)-Ru octahedral nanocrystals exhibit the best performance compared with fcc-Ru truncated cubes, fcc-Ru particles, and conventional hexagonal close-packed (hcp)-Ru particles.

Metal alloy catalysts Although the OER performance of mono-metallic Ir or Ru has achieved some progress, the activity and stability are still far from practical application. Alloying is an outstanding approach to significantly alter the electronic structures and optimize the adsorption energy of reaction intermediates on the catalyst surface, which in turn extremely improves the OER activity. Simultaneously, the alloy strategy could noticeably reduce the usage of precious metals Ir and Ru.

A wide range of Ir-based alloy structures has been synthesized and applied in acidic OER, such as nanodendrite [93, 94], thin film [95], nanowires [64], nanotube [96], and porous structure [65, 97]. For example, a series of IrM (M = Ni, Co, Fe) nanoporous nanowires (IrM NPNWs) were prepared through a novel eutectic-directed self-templating method [64], the subsequent dealloying process introduced the abundant nanoporous structure. The IrM NPNWs after the introduction of Fe, Co, and Ni all have an eminent performance in 0.1 M $HClO_4$, of which the Ni is the most promising element and IrNi NPNWs displays the finest catalytic performance and durability. DFT calculations confirmed that alloy formation can shift down the d-band center and alter the adsorption strength of O-related intermediates, elucidating the relationship between the d-band center and bond strength. Apart from promoting the intrinsic activity of catalysts, increasing the number of active sites is another typical strategy to optimize catalytic performance via morphology and structure control. As shown in Fig. 8a-c, a nanovoid incorporated Ir_3Cu metallic aerogel was formed by a galvanic displacement reaction and gelation process [65]. The electrochemical active surface area (ECSA) derived from the double-layer capacitance of Ir_3Cu is much larger than that of commercial IrO_2 and other counterparts, revealing the much more active sites of Ir_3Cu toward OER. Additionally, the introduction of Cu weakens the binding energy of O-related species and promotes mass transfer. Downsizing the catalyst NPs diameter is also a general method to increase the specific surface area and active sites [66, 67]. A scalable microwave-assisted method was used to prepare the ultrasmall (sub-10 nm) composition-tunable Rh-Ir alloy NPs [67], which displayed a significant enhancement of acidic OER performance to pure Ir NPs. Theoretical studies demonstrated that the introduction of foreign Rh atoms could regulate the electronic structure and strain, which could weaken the adsorption strength of oxygen-containing intermediates. The mass activity of $Rh_{22}Ir_{78}$ NPs could reach 1.17 A mg^{-1}_{Ir} at the overpotential of 300 mV and achieve a threefold increase compared with pure Ir NPs. Ru-based alloys also provided opportunities for optimizing the intrinsic OER activity and improving the stability. For example, combinatorial synthesis and high throughput screening method were used to prepare a series of bimetallic Ru-M (M = Pd, Ir, Cu, Co, Re, Cr, Ni) alloys [98]. The Ru-Co, Ru-Cu, and Ru-Ir exhibited distinctly improved OER activities compared to pure Ru catalyst. Liu and co-workers [68] reported a simple hydrothermal method to synthesize ultrasmall IrRu nanoclusters supported on amorphous tellurium (Te) NPs (IrRu@Te), which was high conductive and acid-stable. This IrRu@Te catalyst displayed distinguished catalytic performance and decent stability, only needing an overpotential of 220 mV to deliver 10 mA cm^{-2}, benefitting from the strong electronic coupling between IrRu nanoclusters and Te, which could effectively reduce the kinetic barrier for OER and prevent the dissolution of IrRu nanoclusters.

In addition to preparing bimetallic alloys, designing ternary or multi-metallic alloys is a plausible approach to altering the electronic environment and increasing the number of surface active sites [69, 73, 99]. A co-reduction polyol method was used to prepare transition-metal (TM) doped RuIr nanocrystals catalysts [69], the introduction of different TMs has a significant effect on the catalytic performance (Fig. 8d-h). To deliver a current density of 10 mA cm^{-2}, the Co-RuIr only required a low overpotential of 235 mV and achieved a long-term chronopotentiometry measurement at 10 mA cm^{-2}. Various multi-metallic-based hollow NPs such as nanoframes and nanocages have been designed and acted as ideal catalysts [70–72], owing to their highly exposed accessible active sites and readily tunable components. A cubic $Pt_{39}Ir_{10}Pd_{11}$ nanocage catalyst was prepared and applied as a bi-functional catalyst toward oxygen reduction reaction (ORR) and OER in acidic media [70], with an average edge length of 12.3 nm and porous walls of 1.0 nm. This catalyst exhibited an unexpected activity and durability ascribed to the highly open structure and electron coupling. Park et al. prepared a robust IrNiCu catalyst with a double-layered nanoframe (DNF) structure. The unique porous morphology endowed it with remarkable activity and stability for acidic OER. This work provided a simple synthetic method for engineering high-active catalysts with complex nanoframe structures.

Metal oxide catalysts Compared to metal catalysts, metal oxide catalysts are more active and stable under acidic and oxidizing OER conditions. Hartig-Weiss et al. [100] reported an Ir oxide catalyst supported on high surface area and high-conductivity antimony-doped tin oxide, which displayed a very compelling OER activity and reduced the usage of Ir metal, benefitting from the uniform catalyst dispersion and strong metal-support interaction (SMSI). The oxidized Ir quantum dots

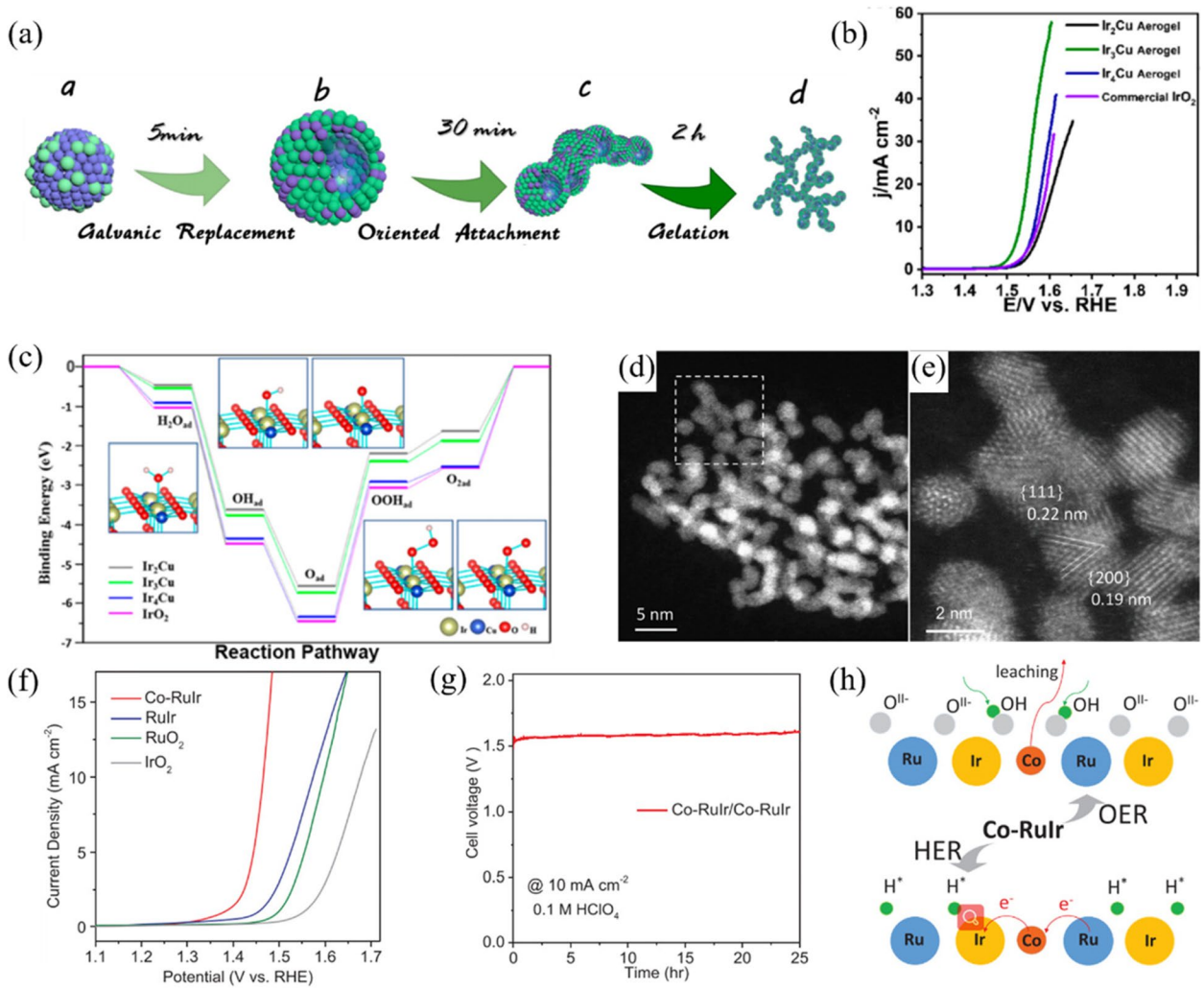

Fig. 8 **a** Schematic illustration of the formation process of Ir_3Cu metallic aerogel. **b** OER curves and (**c**) calculated reaction paths of different Ir_xCu catalysts [65]. **d**,**e** HAADF-STEM images of Co-RuIr nanocrystal. **f** OER LSV curves of Co-RuIr, RuIr, RuO_2, and IrO_2 in 0.1 M $HClO_4$ solution. **g** The long-term continuous overall water splitting for Co-RuIr/Co-RuIr at a current density of 10 mA cm^{-2}. **h** Schematic of catalytic mechanism on Co-RuIr catalyst in acidic media [69]

supported on the surface of graphdiyne (IrO_xQD/GDY) are synthesized and showed incredibly acidic OER performance and robust stability [74], which only need a small overpotential of 236 mV to reach a current density of 10 mA cm^{-2}. In this work, GDY could effectively improve the electrical conductivity, facilitate the charge transfer, easy gas releasing and protect the Ir catalysts from corrosion. The early transition metals have a relatively high resistance to corrosion in strong acids [101], thus, the introduction of early transition metals may have a significant effect on the acidic OER performance. An early transition metal hafnium-modified IrO_x ($IrHf_xO_y$) was successfully prepared and displayed intriguing OER activity in both alkaline and acid electrolytes [75]. In order to improve the OER performance of RuO_x, a low-cost rutile-structured chromium-ruthenium oxide catalyst ($Cr_{0.6}Ru_{0.4}O_2$) was prepared through pyrolysis of Cr-based MOF [76], which unfolded an ultra-low overpotential of 178 mV at 10 mA cm^{-2}, as shown in Fig. 9. Combining XANES results and DFT calculations, they found that the presence of electron transfer from Ru to Cr, and the high valence Ru has the plausible ability for the OER. The introduction of Cr could tailor the electron structure of the RuO_2 phase and has a profound effect on optimizing the durability and activity. It is well known that RuO_2 has relatively higher acidic OER activity derived from its appropriate binding ability of oxygen-contained intermediates, but poor stability. Many reports

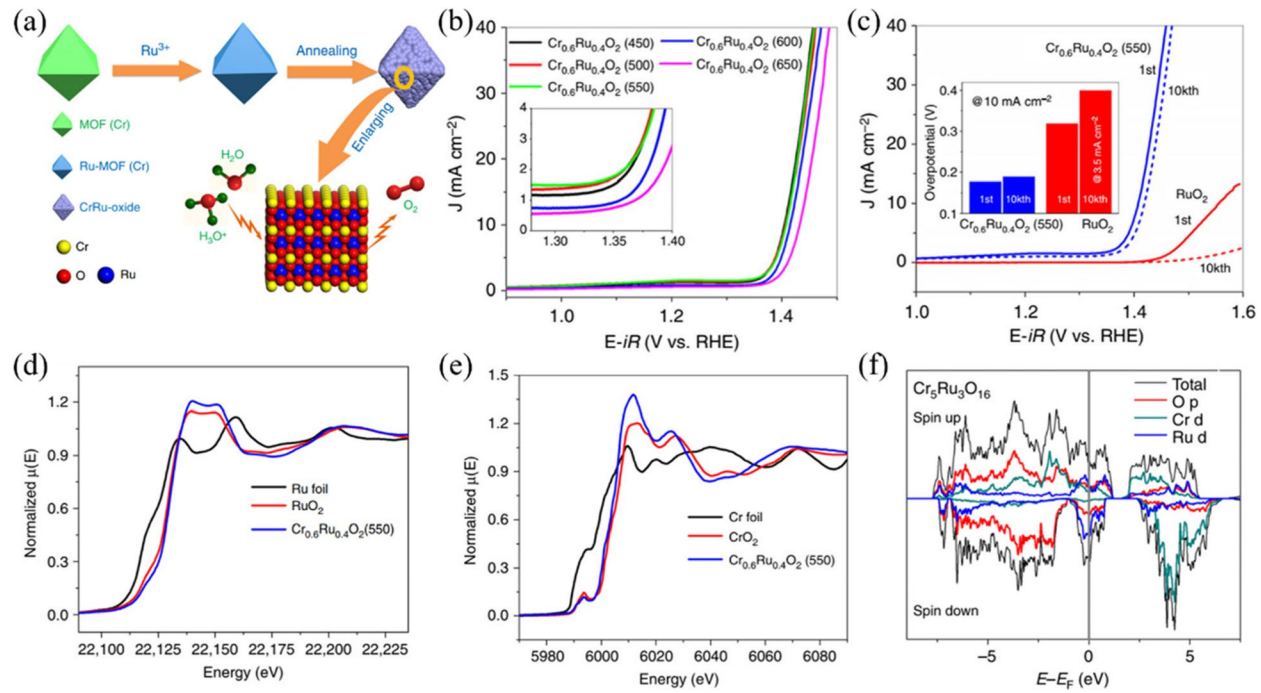

Fig. 9 **a** Schematic route for the synthesis of $Cr_{0.6}Ru_{0.4}O_2$ catalyst. **b** OER activity of $Cr_{0.6}Ru_{0.4}O_2$ annealed at different temperatures. **c** Stability of $Cr_{0.6}Ru_{0.4}O_2$ and commercial RuO_2. **d** Ru and (**e**) Cr K-edge XANES spectra. **f** DOS result of $Cr_5Ru_3O_{16}$ [76]

have demonstrated that the unsatisfactory stability is ascribed to the over-oxidation of Ru-based materials and the formation of the soluble $Ru^{x>4}$ derivatives [77, 102]. In order to improve the stability, Zhang and co-workers [77] prepared a bimetallic-doped RuO_x ($W_{0.2}Er_{0.1}Ru_{0.7}O_{2-\delta}$) catalyst as shown in Fig. 10. They found that the introduction of W and Er elements could modulate the electron structure of RuO_2 and distinctly increase the formation energy of oxygen vacancy, resulting in an excellent durability of up to 500 h in 0.5 M H_2SO_4, as well as unrivalled OER performance. Because the amorphous/crystalline (*a/c*) heterostructure usually unravels unique electronic synergy and exceptionally catalytic performance, Zhang et al. reported a sodium-decorated *a/c*-RuO_2 electrocatalyst [78]. This *a/c*-RuO_2 catalyst displayed a high resistance to acid corrosion and excellent OER activities in all pH environments. Since the relatively higher activity of RuO_2 and much higher stability of IrO_2, preparing IrRu bimetallic oxide or core/shell structure is a promising strategy to form a catalyst with high activity and stability. A highly active and stable $RuIrO_x$ nano-netcage catalyst was reported by Li and co-workers [79] through a dispersing-etching-holing method using MOF as the template. This open nano-netcage structure with abundant mesoporous could simultaneously improve the atom utilization of Ru/Ir and increase the ECSA. With the unique morphology and component, this $RuIrO_x$ catalyst displayed incredibly startling activity with a low overpotential of 233 mV for reaching 10 mA cm^{-2}.

Perovskite oxides have also received much attention in acidic OER due to the low usage of precious metals, compositional flexibility, and structural stability [103, 104]. A pseudocubic $SrCo_{0.9}Ir_{0.1}O_{3-\delta}$ perovskite catalyst with IrO_6 octahedra was designed and prepared [105]. This $SrCo_{0.9}Ir_{0.1}O_{3-\delta}$ catalyst displayed a high turnover frequency of 2.56 ± 0.15 s^{-1} at 1.5 V, which was two orders of magnitude higher than that in the IrO_2 catalyst. They found that the structural reconstruction of $SrCo_{0.9}Ir_{0.1}O_{3-\delta}$ was generated during the anodic oxidation process and accompanied by the Sr and Co elements leaching. Therefore, the catalytic species are corner-shared and under-coordinated IrO_x octahedrons derived from $SrCo_{0.9}Ir_{0.1}O_{3-\delta}$. The alkaline OER is catalyzed by $SrRuO_3$ thin film with relatively higher activity [106], but the performance is poor in acidic OER. Based on this, a Na-doped $SrRuO_3$ ($Sr_{1-x}Na_xRuO_3$) was synthesized by a wet-chemistry procedure [102], which displayed both improved activity and stability in an acidic solution. The enhanced OER mechanism is demonstrated based on XANES and theoretical calculations, Na incorporation increased the valence state of Ru, weakened Ru-adsorbate bonds, and improved the dissolution potentials.

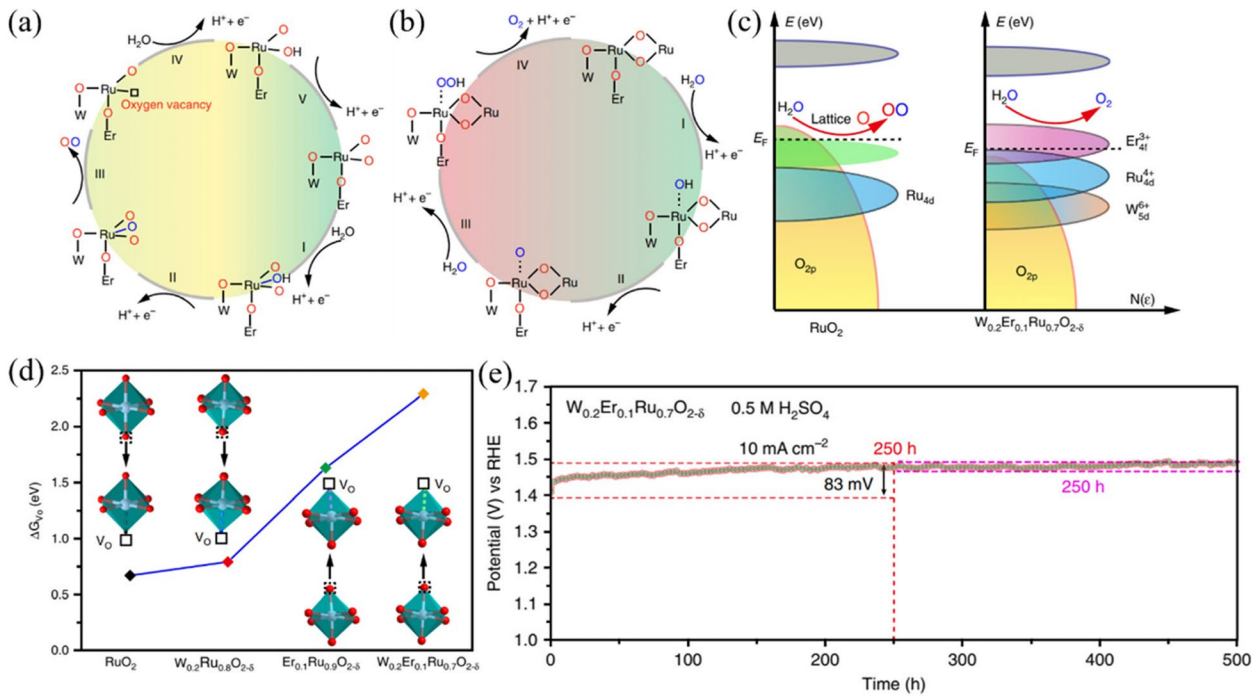

Fig. 10 The illustration of (**a**) lattice oxygen oxidation way and (**b**) adsorbate evolution way of $W_{0.2}Er_{0.1}Ru_{0.7}O_{2-\delta}$ toward acidic OER. **c** Schematic diagrams of rigid band models for RuO_2 and $W_{0.2}Er_{0.1}Ru_{0.7}O_{2-\delta-1}$ toward acidic OER. **d** The calculated energy for the formation of oxygen vacancies. **e** Stability test of $W_{0.2}Er_{0.1}Ru_{0.7}O_{2-\delta}$ at a current density of 10 mA cm^{-2} in 0.5 M H_2SO_4 [77]

4 Other key materials for PEM water electrolysis

As shown in Fig. 11, expect catalysts, other key materials for PME water electrolysis are membrane electrode assembly (MEA), current collector, and bipolar plate. The photograph of the PEM water electrolysis cell assembly is presented in Fig. 11a.

4.1 Membrane electrode assembly (MEA)

The membrane electrode assemblies are made up of proton exchange membrane, ionomer solution, and catalysts. Proton exchange membrane is also called polymer exchange membrane, which plays a critical role in separating product gases, transporting protons, and supporting catalyst layers [12]. The commercial membrane must have advantages of high mechanical strength and proton conductivity, outstanding oxidative and thermal stability. At present, these membranes are mainly focused on perfluorosulfonic acid polymer membranes, such as Nafion, Fumapem, and Flemion. However, the most commonly used are Nafion membranes (Nafion 115, 117, and 212)

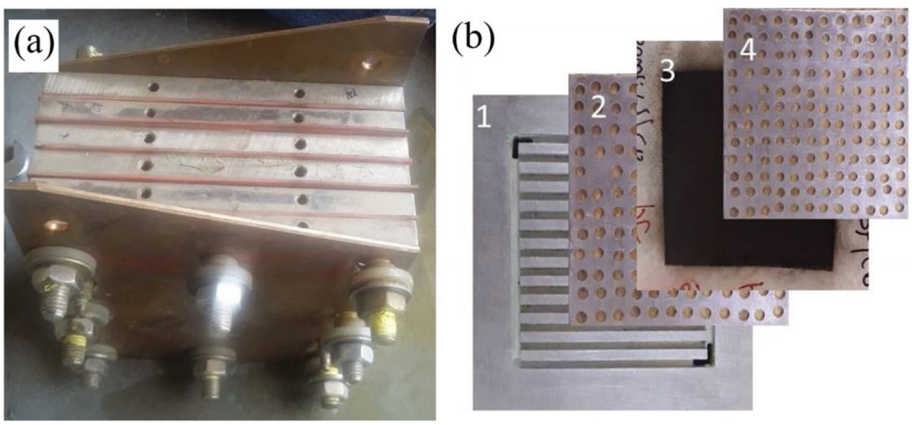

Fig. 11 **a** PEM cell stack. **b** Cell components, 1-Bipolar plate, 2-Anode current collector, 3-MEA, 4-Cathode current collector [12]

in PEM water electrolysers because of the advantages of high proton conductivity, high durability at higher current densities (2 A cm^{-2}), but the high price and complex disposal when disused restrict its development. Research efforts have been devoted to reducing the cost of these polymer membranes and simultaneously optimizing the ion exchange characteristics and stability. In order to improve the performance of PEM and reduce the cost, the enhanced composite scheme can be used to improve the mechanical properties of PEM, which is beneficial to reduce the thickness of the membrane. Moreover, the membrane resistance and electrolytic energy can be reduced by increasing the ionic conductivity of the film, which is beneficial to improving the overall performance of the electrolyser. According to the different catalyst layer supports, membrane electrode preparation methods consist of the catalyst-coating substrate (CCS) method and catalyst-coating membrane (CCM) method. The CCS method directly coats the catalyst active components on the gas diffusion layer, while the CCM method directly coats the catalyst active components on both sides of the proton exchange membrane, which is the biggest difference between the two manufacturing processes. Compared with the CCS method, the CCM method has a higher catalyst utilization rate and greatly reduces the proton transfer resistance between the membrane and the catalytic layer. CCM is the most common method to prepare MEAs. In this process, the homogeneous catalyst slurry, which was performed by sonication of a mixture of catalysts, ionomer solution, and solvent, is directly coated on the membrane and hot-pressed at high pressure [107]. The sputtering method, spraying method, electrochemical deposition and decal method are usually used in the CCS and CCM methods.

4.2 Current collector

Current collectors are porous media placed between the MEA and bipolar plate at both electrode sides. In PEM water electrolysers, water is usually input on the anode side of the cell, where the OER takes place. The water diffuses through the channels in the separation plate and through the current collectors. The major functions are electric conduction between the electrode and the bipolar plate, as well as transport of liquid/gas from the reaction site with as low as activation, thermal, ohmic, and fluidic losses [108]. The current collector should have energetic corrosion resistance and super electrical conductivity because of the strong acidic media and strongly oxidative environments. Additionally, the pore size and structure of the current collector are important, because the produced gases in the PEM water electrolysis process should be effectively expelled and water must be reaching the catalytic sites of the electrode surface [109]. The porous titanium plates are the most used current collectors for both sides of MEA due to their decent conductivity, excellent mechanical stability, and corrosion resistance.

4.3 Bipolar plate

Bipolar plate is an essential component in the PEM electrolyser stack, reducing the cost of bipolar plates is the key to controlling the cost of electrolysers. In the harsh working environment of the anode of the PEM electrolytic cell, if the bipolar plate is corroded, it will lead to the leaching of metal ions, thereby contaminating the PEM system. Therefore, the commonly used bipolar plate protection measure is to prepare a layer of anti-corrosion coating on the surface. The bipolar plates play multifunctional roles, such as separators, conduct heat and current between single cells in a stack, heat and water management [110]. Thus, the bipolar plate must have excellent strength, high thermal conductivity, low permeability, and high shock durability. Graphite has been previously used as a bipolar plate due to its excellent electrical conductivity. Nevertheless, there are many problems including the high corrosion rates, depressed mechanical strength, and exorbitant cost. Currently, the most commonly used bipolar plates are titanium and coated stainless steel [111, 112]. But there are still some challenges, such as hydrogen embrittlement, passivation, and corrosion [113]. Therefore, exploiting cost-effective and stable bipolar plates is still under challenge.

5 Conclusions and prospects

In summary, hydrogen is considered as an environmentally benign alternative to traditional fossil fuels due to its high energy density and carbon-free pollution. AWE, SOE, and PEM water electrolysis are the main electrolysis technologies for hydrogen production. PEM water electrolysis is hailed as the most desired technology for high purity hydrogen production and self-consistent with volatility of renewable energies. From the thorough overview of the recent development of acidic HER and OER electrocatalysts for water splitting, there still exist many obstacles to exploiting and studying high-efficiency electrocatalysts. These are summarized as follows:

1) Pt and Pt-based catalysts are still the most popular materials for acidic HER. Numerous studies have made great processes in improving the activity and stability by using nonprecious metals, but the performance still fails to meet the requirement of practical electrolysers. In order to optimize the catalytic performance, compositional modulation, downsizing, and tailoring the electronic structure are effective

strategies to increase the intrinsic activity and density of catalytically active sites.

2) OER catalyst for PEM is mainly focused on IrO_2 with high stability. However, the relatively low activity and the exorbitant cost severely restrain the practical applications. Compared with IrO_2, although Ru-based catalysts exhibited high activity and low price, the over-oxidation in acidic electrolytes resulted in poor stability. More attention needs to be paid to optimizing the activity of IrO_2 and improving the stability of Ru-based catalysts.
3) The catalytic processes in PEM electrolyser, especially for acidic OER, still have no well-established reaction mechanism. To discover the reaction mechanism on catalytic sites and monitor the dynamic evolution of the catalyst during the reaction process, advanced operando/in situ technologies are needed. For example, operando XAFS, Raman, XRD, and FTIR spectra, could explore the morphology, composition, and crystal structure change, as well as identification of real active sites, during the long-term electrolysis. In addition, the theoretical calculation is a critical tool to investigate the reaction pathways and unravel the catalysis mechanism.
4) The remarkable catalyst for industrial application needs higher current densities while maintaining a low operating voltage. Such commercial PEM water electrolysis requires a long operation time at high current densities of 2–3 A cm^{-2} for high energy conversion efficiency. However, such higher current densities usually need relatively high operating voltage, most catalysts are unstable during the OER process in acidic media. Much more effort should be devoted to exploring the functional links between stability and activity.

Abbreviations
PEM: Proton exchange membrane; AWE: Alkaline water electrolysis; SOE: Solid oxide electrolysis; HER: Hydrogen evolution reaction; OER: Oxygen evolution reaction; TMDs: Transition metal dichalcogenides; TMPs: Transition metal phosphides; TMCs: Transition metal carbides; MEA: Membrane electrode assembly; DFT: Density functional theory; SACs: Single atom catalysts.

Acknowledgements
Not applicable.

Authors' information
Tongzhou Wang is a Ph.D. student in the group of Prof. Lifang Jiao at Nankai University, China. His current research focus on the design and fabrication of high-performance electrode material for electrolysis and energy devices.
Xuejie Cao is a Ph.D. student in the group of Prof. Lifang Jiao at Nankai University, China. Her current research focus on the rational design and fabrication of high-performance nanomaterial for water splitting.
Lifang Jiao is currently a Professor at Nankai University, China. She received her PhD degree from Nankai University (China) in 2005. Her current research is focused on energy conversion and storage, and electrocatalytic hydrogen evolution.

Authors' contributions
TZ and XJ prepared the manuscript, LF gave helpful comments and suggestions. All authors read and approved the final manuscript.

Funding
This work was financially supported by National Key R&D Program of China (2021YFB4000200), the National Natural Science Foundation of China (52025013, 51622102), Haihe Laboratory of Sustainable Chemical Transformations, the 111 Project (B12015), and the Fundamental Research Funds for the Central Universities.

Availability of data and material
Not applicable.

Declarations

Ethics approval and consent to participate
Not applicable.

Consent for publication
Yes.

Competing interests
The authors declare that they have no conflict of interest.

Author details
[1]Key Laboratory of Advanced Energy Materials Chemistry (Ministry of Education), Renewable Energy Conversion and Storage Center (RECAST), College of Chemistry, Nankai University, Tianjin 300071, China. [2]Haihe Laboratory of Sustainable Chemical Transformations, Tianjin 300192, China.

Received: 28 December 2021 Accepted: 13 May 2022
Published online: 02 June 2022

References

1. Zhu J, Hu LS, Zhao PX, Lee LYS, Wong K-Y (2020) Recent Advances in Electrocatalytic Hydrogen Evolution Using Nanoparticles. Chem Rev 120:851–918
2. Li L, Wang P, Shao Q, Huang X (2020) Metallic nanostructures with low dimensionality for electrochemical water splitting. Chem Soc Rev 49:3072–3106
3. Wang T, Cao X, Jiao L (2021) MOFs-Derived Carbon-Based Metal Catalysts for Energy-Related Electrocatalysis. Small 17:2004398
4. Tian X, Zhao P, Sheng W (2019) Hydrogen Evolution and Oxidation: Mechanistic Studies and Material Advances. Adv Mater 31:1808066
5. Chi J, Yu H (2018) Water electrolysis based on renewable energy for hydrogen production. Chinese J Catal 39:390–394
6. Yang L, Qin H, Dong Z, Wang T, Wang G, Jiao L (2021) Metallic S-CoTe with Surface Reconstruction Activated by Electrochemical Oxidation for Oxygen Evolution Catalysis. Small 17:2102027
7. Zhang H, Maijenburg AW, Li X, Schweizer SL, Wehrspohn RB (2020) Bifunctional Heterostructured Transition Metal Phosphides for Efficient Electrochemical Water Splitting. Adv Funct Mater 30:2003261
8. Cao X, Wang T, Jiao L (2021) Transition-Metal (Fe Co, and Ni)-Based Nanofiber Electrocatalysts for Water Splitting. Adv Fiber Mater 3:210–228
9. Peng Y, Lu B, Chen S (2018) Carbon-Supported Single Atom Catalysts for Electrochemical Energy Conversion and Storage. Adv Mater 30:1801995
10. Guo X, Wan X, Liu Q, Li Y, Li W, Shui J (2022) Phosphated IrMo bimetallic cluster for efficient hydrogen evolution reaction. eScience https://doi.org/10.1016/j.esci.2022.04.002
11. Prieto G, Tuysuz H, Duyckaerts N, Knossalla J, Wang GH, Schuth F (2016) Hollow Nano- and Microstructures as Catalysts. Chem Rev 116:14056–14119
12. Marshall A, Børresen B, Hagen G, Tsypkin M, Tunold R (2007) Hydrogen production by advanced proton exchange membrane (PEM) water

electrolysers—Reduced energy consumption by improved electrocatalysis. Energy 32:431–436
13. Lewinski KA, van der Vliet DF, Luopa SM (2015) NSTF Advances for PEM Electrolysis-The Effect of Alloying on Activity of NSTF Electrolyzer Catalysts and Performance of NSTF Based PEM Electrolyzers. ECS Trans 69:893–917
14. Shiva Kumar S, Himabindu V (2019) Hydrogen production by PEM water electrolysis – A review. Mater Sci Energy Technol 2:442–454
15. Carmo M, Fritz DL, Mergel J, Stolten D (2013) A comprehensive review on PEM water electrolysis. Int J Hydrogen Energy 38:4901–4934
16. Bi L, Boulfrad S, Traversa E (2014) Steam electrolysis by solid oxide electrolysis cells (SOECs) with proton-conducting oxides. Chem Soc Rev 43:8255–8270
17. Xu W, Scott K (2010) The effects of ionomer content on PEM water electrolyser membrane electrode assembly performance. Int J Hydrogen Energy 35:12029–12037
18. Siracusano S, Baglio V, Lufrano F, Staiti P, Aricò AS (2013) Electrochemical characterization of a PEM water electrolyzer based on a sulfonated polysulfone membrane. J Membr Sci 448:209–214
19. Eiler K, Suriñach S, Sort J, Pellicer E (2020) Mesoporous Ni-rich Ni–Pt thin films: Electrodeposition, characterization and performance toward hydrogen evolution reaction in acidic media. Appl Catal, B Environ. 265:118597
20. Ayers KE, Renner JN, Danilovic N, Wang JX, Zhang Y, Maric R, Yu H (2016) Pathways to ultra-low platinum group metal catalyst loading in proton exchange membrane electrolyzers. Catal Today 262:121–132
21. Zhong W, Tu W, Wang Z, Lin Z, Xu A, Ye X, Chen D, Xiao B (2020) Ultralow-temperature assisted synthesis of single platinum atoms anchored on carbon nanotubes for efficiently electrocatalytic acidic hydrogen evolution. J Energy Chem 51:280–284
22. Xu J, Zhang C, Liu H, Sun J, Xie R, Qiu Y, Lü F, Liu Y, Zhuo L, Liu X, Luo J (2020) Amorphous MoO_x-Stabilized single platinum atoms with ultrahigh mass activity for acidic hydrogen evolution. Nano Energy 70:104529
23. Ramakrishna SUB, Srinivasulu Reddy D, Shiva Kumar S, Himabindu V (2016) Nitrogen doped CNTs supported Palladium electrocatalyst for hydrogen evolution reaction in PEM water electrolyser. Int J Hydrogen Energy 41:20447–20454
24. Morozan A, Johnson H, Roiron C, Genay G, Aldakov D, Ghedjatti A, Nguyen CT, Tran PD, Kinge S, Artero V (2020) Nonprecious Bimetallic Iron-Molybdenum Sulfide Electrocatalysts for the Hydrogen Evolution Reaction in Proton Exchange Membrane Electrolyzers. ACS Catal 10:14336–14348
25. Hinnemann B, Moses PG, Bonde J, Jørgensen KP, Nielsen JH, Horch S, Chorkendorff I, Nørskov JK (2005) Biomimetic Hydrogen Evolution: MoS_2 Nanoparticles as Catalyst for Hydrogen Evolution. J Am Chem Soc 127:5308–5309
26. Yang C, Zhao R, Xiang H, Wu J, Zhong W, Li W, Zhang Q, Yang N, Li X (2020) Ni-Activated Transition Metal Carbides for Efficient Hydrogen Evolution in Acidic and Alkaline Solutions. Adv Energy Mater 10:2002260
27. Hu K, Ohto T, Nagata Y, Wakisaka M, Aoki Y, Fujita JI, Ito Y (2021) Catalytic activity of graphene-covered non-noble metals governed by proton penetration in electrochemical hydrogen evolution reaction. Nat Commun 12:203
28. Yoo S, Kim Y, Yoon Y, Karuppannan M, Kwon OJ, Lim T (2021) Encapsulation of Pt nanocatalyst with N-containing carbon layer for improving catalytic activity and stability in the hydrogen evolution reaction. Int J Hydrogen Energy 46:21454–21461
29. Feng G, Ning F, Song J, Shang H, Zhang K, Ding Z, Gao P, Chu W, Xia D (2021) Sub-2 nm Ultrasmall High-Entropy Alloy Nanoparticles for Extremely Superior Electrocatalytic Hydrogen Evolution. J Am Chem Soc 143:17117–17127
30. Lu Q, Yu Y, Ma Q, Chen B, Zhang H (2016) 2D Transition-Metal-Dichalcogenide-Nanosheet-Based Composites for Photocatalytic and Electrocatalytic Hydrogen Evolution Reactions. Adv Mater 28:1917–1933
31. Liu Z, Gao Z, Liu Y, Xia M, Wang R, Li N (2017) Heterogeneous Nanostructure Based on 1T-Phase MoS_2 for Enhanced Electrocatalytic Hydrogen Evolution. ACS Appl Mater Interfaces 9:25291–25297
32. Sun T, Wang J, Chi X, Lin Y, Chen Z, Ling X, Qiu C, Xu Y, Song L, Chen W, Su C (2018) Engineering the Electronic Structure of MoS_2 Nanorods by N and Mn Dopants for Ultra-Efficient Hydrogen Production. ACS Catal 8:7585–7592
33. Zhao Z, Qin F, Kasiraju S, Xie L, Alam MK, Chen S, Wang D, Ren Z, Wang Z, Grabow LC, Bao J (2017) Vertically Aligned MoS_2/Mo_2C hybrid Nanosheets Grown on Carbon Paper for Efficient Electrocatalytic Hydrogen Evolution. ACS Catal 7:7312–7318
34. Luo Y, Zhang S, Pan H, Xiao S, Guo Z, Tang L, Khan U, Ding BF, Li M, Cai Z, Zhao Y, Lv W, Feng Q, Zou X, Lin J, Cheng HM, Liu B (2020) Unsaturated Single Atoms on Monolayer Transition Metal Dichalcogenides for Ultrafast Hydrogen Evolution. ACS Nano 14:767–776
35. Cheng Y, Lu S, Liao F, Liu L, Li Y, Shao M (2017) Rh-MoS_2 Nanocomposite Catalysts with Pt-Like Activity for Hydrogen Evolution Reaction. Adv Funct Mater 27:1700359
36. Zhang Z, Xu J, Wen Y, Wang T (2018) A highly-sensitive VB_2 electrochemical sensor based on one-step co-electrodeposited molecularly imprinted WS_2-PEDOT film supported on graphene oxide-SWCNTs nanocomposite. Mater Sci Eng C 92:77–87
37. Deng S, Yang F, Zhang Q, Zhong Y, Zeng Y, Lin S, Wang X, Lu X, Wang CZ, Gu L, Xia X, Tu J (2018) Phase Modulation of (1T–2H)-$MoSe_2$/TiC-C Shell/Core Arrays via Nitrogen Doping for Highly Efficient Hydrogen Evolution Reaction. Adv Mater 30:1802223
38. Zhang C, Chen X, Peng Z, Fu X, Lian L, Luo W, Zhang J, Li H, Wang Y, Zhang D (2018) Phosphine-free synthesis and shape evolution of $MoSe_2$ nanoflowers for electrocatalytic hydrogen evolution reactions. CrystEngComm 20:2491–2498
39. Chen W, Qiao R, Song C, Zhao L, Jiang Z-J, Maiyalagan T, Jiang Z (2020) Tailoring the thickness of $MoSe_2$ layer of the hierarchical double-shelled N-doped carbon@$MoSe_2$ hollow nanoboxes for efficient and stable hydrogen evolution reaction. J Catal 381:363–373
40. Tsai C, Chan K, Abild-Pedersen F, Norskov JK (2014) Active edge sites in $MoSe_2$ and WSe_2 catalysts for the hydrogen evolution reaction: a density functional study. Phys Chem Chem Phys 16:13156–13164
41. Kim JH, Kim H, Kim J, Lee HJ, Jang JH, Ahn SH (2018) Electrodeposited molybdenum sulfide as a cathode for proton exchange membrane water electrolyzer. J Power Sources 392:69–78
42. Wang T, Liu C, Wang X, Li X, Jiang F, Li C, Hou J, Xu J (2017) Highly enhanced thermoelectric performance of WS_2 nanosheets upon embedding PEDOT:PSS. J Polym Sci B Polym Phys 55:997–1004
43. Wang T, Liu C, Xu J, Zhu Z, Liu E, Hu Y, Li C, Jiang F (2016) Thermoelectric performance of restacked MoS_2 nanosheets thin-film. Nanotechnology 27:285703
44. Wang T, Liu C, Jiang F, Xu Z, Wang X, Li X, Li C, Xu J, Yang X (2017) Solution-processed two-dimensional layered heterostructure thin-film with optimized thermoelectric performance. Phys Chem Chem Phys 19:17560–17567
45. Kwon IS, Kwak IH, Debela TT, Kim JY, Yoo SJ, Kim JG, Park J, Kang HS (2021) Phase-Transition $Mo_{1-x}V_xSe_2$ Alloy Nanosheets with Rich V-Se Vacancies and Their Enhanced Catalytic Performance of Hydrogen Evolution Reaction. ACS Nano 15:14672–14682
46. Zhang B, Wang J, Liu J, Zhang L, Wan H, Miao L, Jiang J (2019) Dual-Descriptor Tailoring: The Hydroxyl Adsorption Energy-Dependent Hydrogen Evolution Kinetics of High-Valance State Doped Ni_3N in Alkaline Media. ACS Catal 9:9332–9338
47. Wang T, Cao X, Qin H, Chen X, Li J, Jiao L (2021) Integrating energy-saving hydrogen production with methanol electrooxidation over Mo modified Co_4N nanoarrays. J Mater Chem A 9:21094–21100
48. Zhao Y, Hwang J, Tang MT, Chun H, Wang X, Zhao H, Chan K, Han B, Gao P, Li H (2020) Ultrastable molybdenum disulfide-based electrocatalyst for hydrogen evolution in acidic media. J Power Sources 456:227998
49. Gu X, Yang X, Feng L (2020) An Efficient $RuTe_2$/Graphene Catalyst for Electrochemical Hydrogen Evolution Reaction in Acid Electrolyte. Chem Asian J 15:2886–2891
50. Sapountzi FM, Orlova ED, Sousa JPS, Salonen LM, Lebedev OI, Zafeiropoulos G, Tsampas MN, Niemantsverdriet HJW, Kolen'ko, Y. V. (2020) FeP Nanocatalyst with Preferential [010] Orientation Boosts the Hydrogen Evolution Reaction in Polymer-Electrolyte Membrane Electrolyzer. Energy Fuels 34:6423–6429
51. Shiva Kumar S, Himabindu V (2020) Boron-Doped Carbon nanoparticles supported palladium as an efficient hydrogen evolution electrode in PEM water electrolysis. Renewable Energy 146:2281–2290

52. Fu L, Zeng X, Huang C, Cai P, Cheng G, Luo W (2018) Ultrasmall Ir nanoparticles for efficient acidic electrochemical water splitting. Inorg Chem Front 5:1121–1125
53. Xue Q, Gao W, Zhu J, Peng R, Xu Q, Chen P, Chen Y (2018) Carbon nanobowls supported ultrafine iridium nanocrystals: An active and stable electrocatalyst for the oxygen evolution reaction in acidic media. J Colloid Interface Sci 529:325–331
54. Luo F, Hu H, Zhao X, Yang Z, Zhang Q, Xu J, Kaneko T, Yoshida Y, Zhu C, Cai W (2020) Robust and Stable Acidic Overall Water Splitting on Ir Single Atoms. Nano Lett 20:2120–2128
55. Shan J, Ye C, Chen S, Sun T, Jiao Y, Liu L, Zhu C, Song L, Han Y, Jaroniec M, Zhu Y, Zheng Y, Qiao SZ (2021) Short-Range Ordered Iridium Single Atoms Integrated into Cobalt Oxide Spinel Structure for Highly Efficient Electrocatalytic Water Oxidation. J Am Chem Soc 143:5201–5211
56. Pi Y, Zhang N, Guo S, Guo J, Huang X (2016) Ultrathin Laminar Ir Superstructure as Highly Efficient Oxygen Evolution Electrocatalyst in Broad pH Range. Nano Lett 16:4424–4430
57. Jiang B, Wang T, Cheng Y, Liao F, Wu K, Shao M (2018) Ir/g-C_3N_4/Nitrogen-Doped Graphene Nanocomposites as Bifunctional Electrocatalysts for Overall Water Splitting in Acidic Electrolytes. ACS Appl Mater Interfaces 10:39161–39167
58. Jiang B, Guo Y, Kim J, Whitten AE, Wood K, Kani K, Rowan AE, Henzie J, Yamauchi Y (2018) Mesoporous Metallic Iridium Nanosheets. J Am Chem Soc 140:12434–12441
59. Wu G, Zheng X, Cui P, Jiang H, Wang X, Qu Y, Chen W, Lin Y, Li H, Han X, Hu Y, Liu P, Zhang Q, Ge J, Yao Y, Sun R, Wu Y, Gu L, Hong X, Li Y (2019) A general synthesis approach for amorphous noble metal nanosheets. Nat Commun 10:4855
60. Cao L, Luo Q, Chen J, Wang L, Lin Y, Wang H, Liu X, Shen X, Zhang W, Liu W, Qi Z, Jiang Z, Yang J, Yao T (2019) Dynamic oxygen adsorption on single-atomic Ruthenium catalyst with high performance for acidic oxygen evolution reaction. Nat Commun 10:4849
61. Yao Y, Hu S, Chen W, Huang Z-Q, Wei W, Yao T, Liu R, Zang K, Wang X, Wu G, Yuan W, Yuan T, Zhu B, Liu W, Li Z, He D, Xue Z, Wang Y, Zheng X, Dong J, Chang C-R, Chen Y, Hong X, Luo J, Wei S, Li W-X, Strasser P, Wu Y, Li Y (2019) Engineering the electronic structure of single atom Ru sites via compressive strain boosts acidic water oxidation electrocatalysis. Nat Catal 2:304–313
62. Zhu J, Guo Y, Liu F, Xu H, Gong L, Shi W, Chen D, Wang P, Yang Y, Zhang C, Wu J, Luo J, Mu S (2021) Regulative Electronic States around Ruthenium/Ruthenium Disulphide Heterointerfaces for Efficient Water Splitting in Acidic Media. Angew Chem Int Ed 60:12328–12334
63. Zhao M, Chen Z, Lyu Z, Hood ZD, Xie M, Vara M, Chi M, Xia Y (2019) Ru Octahedral Nanocrystals with a Face-Centered Cubic Structure, 111 Facets, Thermal Stability up to 400 degrees C, and Enhanced Catalytic Activity. J Am Chem Soc 141:7028–7036
64. Wang Y, Zhang L, Yin K, Zhang J, Gao H, Liu N, Peng Z, Zhang Z (2019) Nanoporous Iridium-Based Alloy Nanowires as Highly Efficient Electrocatalysts Toward Acidic Oxygen Evolution Reaction. ACS Appl Mater Interfaces 11:39728–39736
65. Shi Q, Zhu C, Zhong H, Su D, Li N, Engelhard MH, Xia H, Zhang Q, Feng S, Beckman SP, Du D, Lin Y (2018) Nanovoid Incorporated IrxCu Metallic Aerogels for Oxygen Evolution Reaction Catalysis. ACS Energy Lett 3:2038–2044
66. Pi Y, Shao Q, Wang P, Guo J, Huang X (2017) General Formation of Monodisperse IrM (M = Ni Co, Fe) Bimetallic Nanoclusters as Bifunctional Electrocatalysts for Acidic Overall Water Splitting. Adv Funct Mater 27:1700886
67. Guo H, Fang Z, Li H, Fernandez D, Henkelman G, Humphrey SM, Yu G (2019) Rational Design of Rhodium-Iridium Alloy Nanoparticles as Highly Active Catalysts for Acidic Oxygen Evolution. ACS Nano 13:13225–13234
68. Xu J, Lian Z, Wei B, Li Y, Bondarchuk O, Zhang N, Yu Z, Araujo A, Amorim I, Wang Z, Li B, Liu L (2020) Strong Electronic Coupling between Ultrafine Iridium-Ruthenium Nanoclusters and Conductive, Acid-Stable Tellurium Nanoparticle Support for Efficient and Durable Oxygen Evolution in Acidic and Neutral Media. ACS Catal 10:3571–3579
69. Shan J, Ling T, Davey K, Zheng Y, Qiao SZ (2019) Transition-Metal-Doped RuIr Bifunctional Nanocrystals for Overall Water Splitting in Acidic Environments. Adv Mater 31:1900510
70. Zhu J, Xie M, Chen Z, Lyu Z, Chi M, Jin W, Xia Y (2020) Pt-Ir-Pd Trimetallic Nanocages as a Dual Catalyst for Efficient Oxygen Reduction and Evolution Reactions in Acidic Media. Adv Energy Mater 10:1904114
71. Park J, Sa YJ, Baik H, Kwon T, Joo SH, Lee K (2017) Iridium-Based Multimetallic Nanoframe@Nanoframe Structure: An Efficient and Robust Electrocatalyst toward Oxygen Evolution Reaction. ACS Nano 11:5500–5509
72. Kwon T, Hwang H, Sa YJ, Park J, Baik H, Joo SH, Lee K (2017) Cobalt Assisted Synthesis of IrCu Hollow Octahedral Nanocages as Highly Active Electrocatalysts toward Oxygen Evolution Reaction. Adv Funct Mater 27:1604688
73. Feng J, Lv F, Zhang W, Li P, Wang K, Yang C, Wang B, Yang Y, Zhou J, Lin F, Wang GC, Guo S (2017) Iridium-Based Multimetallic Porous Hollow Nanocrystals for Efficient Overall-Water-Splitting Catalysis. Adv Mater 29:1703798
74. Wang Z, Zheng Z, Xue Y, He F, Li Y (2021) Acidic Water Oxidation on Quantum Dots of IrOx/Graphdiyne. Adv Energy Mater 11:2101138
75. Zhao F, Wen B, Niu W, Chen Z, Yan C, Selloni A, Tully CG, Yang X, Koel BE (2021) Increasing Iridium Oxide Activity for the Oxygen Evolution Reaction with Hafnium Modification. J Am Chem Soc 143:15616–15623
76. Lin Y, Tian Z, Zhang L, Ma J, Jiang Z, Deibert BJ, Ge R, Chen L (2019) Chromium-ruthenium oxide solid solution electrocatalyst for highly efficient oxygen evolution reaction in acidic media. Nat Commun 10:162
77. Hao S, Liu M, Pan J, Liu X, Tan X, Xu N, He Y, Lei L, Zhang X (2020) Dopants fixation of Ruthenium for boosting acidic oxygen evolution stability and activity. Nat Commun 11:5368
78. Zhang L, Jang H, Liu H, Kim MG, Yang D, Liu S, Liu X, Cho J (2021) Sodium-Decorated Amorphous/Crystalline RuO_2 with Rich Oxygen Vacancies: A Robust pH-Universal Oxygen Evolution Electrocatalyst. Angew Chem Int Ed 60:18821–18829
79. Zhuang Z, Wang Y, Xu CQ, Liu S, Chen C, Peng Q, Zhuang Z, Xiao H, Pan Y, Lu S, Yu R, Cheong WC, Cao X, Wu K, Sun K, Wang Y, Wang D, Li J, Li Y (2019) Three-dimensional open nano-netcage electrocatalysts for efficient pH-universal overall water splitting. Nat Commun 10:4875
80. Yang H, Liu Y, Liu X, Wang X, Tian H, Waterhouse G, Kruger P, Telfer S, Ma S (2022) Large-scale synthesis of N-doped carbon capsules supporting atomically dispersed iron for efficient oxygen reduction reaction electrocatalysis. eScience 2:227–234
81. Lin F, Dong Z, Yao Y, Yang L, Fang F, Jiao L (2020) Electrocatalytic Hydrogen Evolution of Ultrathin Co-Mo_5N_6 Heterojunction with Interfacial Electron Redistribution. Adv Energy Mater 10:2002176
82. Su H, Soldatov M, Roldugin V, Liu Q (2022) Platinum single-atom catalyst with self-adjustable valence state for largecurrent-density acidic water oxidation. eScience 2:102–109
83. Wang T, Cao X, Qin H, Shang L, Zheng S, Fang F, Jiao L (2021) P-Block Atomically Dispersed Antimony Catalyst for Highly Efficient Oxygen Reduction Reaction. Angew Chem Int Ed 60:21237–21241
84. Wang T, Wang Q, Wang Y, Da Y, Zhou W, Shao Y, Li D, Zhan S, Yuan J, Wang H (2019) Atomically Dispersed Semimetallic Selenium on Porous Carbon Membrane as an Electrode for Hydrazine Fuel Cells. Angew Chem Int Ed 58:13466–13471
85. Velasco-Vélez JJ, Jones TE, Streibel V, Hävecker M, Chuang CH, Frevel L, Plodinec M, Centeno A, Zurutuza A, Wang R, Arrigo R, Mom R, Hofmann S, Schlögl R, Knop-Gericke A (2019) Electrochemically active Ir NPs on graphene for OER in acidic aqueous electrolyte investigated by in situ and ex situ spectroscopies. Surf Sci 681:1–8
86. Boshnakova I, Lefterova E, Slavcheva E (2018) Investigation of montmorillonite as carrier for OER. Int J Hydrogen Energy 43:16897–16904
87. Dong Z, Lin F, Yao Y, Jiao L (2019) Crystalline Ni$(OH)_2$/Amorphous $NiMoO_x$ Mixed-Catalyst with Pt-Like Performance for Hydrogen Production. Adv Energy Mater 9:1902703
88. Gong Z, Liu R, Gong H, Ye G, Liu J, Dong J, Liao J, Yan M, Liu J, Huang K, Xing L, Liang J, He Y, Fei H (2021) Constructing a Graphene-Encapsulated Amorphous/Crystalline Heterophase NiFe Alloy by Microwave Thermal Shock for Boosting the Oxygen Evolution Reaction. ACS Catal 11:12284–12292
89. Kong X, Xu K, Zhang C, Dai J, Norooz Oliaee S, Li L, Zeng X, Wu C, Peng Z (2016) Free-Standing Two-Dimensional Ru Nanosheets with High Activity toward Water Splitting. ACS Catal 6:1487–1492

90. Kim JY, Choi J, Kim HY, Hwang E, Kim H-J, Ahn SH, Kim S-K (2015) Activity and stability of the oxygen evolution reaction on electrodeposited Ru and its thermal oxides. Appl Surf Sci 359:227–235
91. Lin F, Qin H, Wang T, Yang L, Cao X, Jiao L (2021) Few-layered MoN–MnO heterostructures with interfacial-O synergistic active centers boosting electrocatalytic hydrogen evolution. J Mater Chem A 9:8325–8331
92. Wang T, Cao X, Jiao L (2021) Ni_2P/NiMoP heterostructure as a bifunctional electrocatalyst for energy-saving hydrogen production. eScience 1:69–74
93. Fu L, Zeng X, Cheng G, Luo W (2018) IrCo Nanodendrite as an Efficient Bifunctional Electrocatalyst for Overall Water Splitting under Acidic Conditions. ACS Appl Mater Interfaces 10:24993–24998
94. Zhang G, Shao Z-G, Lu W, Li G, Liu F, Yi B (2012) One-pot synthesis of Ir@Pt nanodendrites as highly active bifunctional electrocatalysts for oxygen reduction and oxygen evolution in acidic medium. Electrochem Commun 22:145–148
95. Strickler AL, Flores RA, King LA, Norskov JK, Bajdich M, Jaramillo TF (2019) Systematic Investigation of Iridium-Based Bimetallic Thin Film Catalysts for the Oxygen Evolution Reaction in Acidic Media. ACS Appl Mater Interfaces 11:34059–34066
96. Zhu M, Shao Q, Qian Y, Huang X (2019) Superior overall water splitting electrocatalysis in acidic conditions enabled by bimetallic Ir-Ag nanotubes. Nano Energy 56:330–337
97. Pi Y, Guo J, Shao Q, Huang X (2018) Highly Efficient Acidic Oxygen Evolution Electrocatalysis Enabled by Porous Ir–Cu Nanocrystals with Three-Dimensional Electrocatalytic Surfaces. Chem Mater 30:8571–8578
98. Forgie R, Bugosh G, Neyerlin KC, Liu Z, Strasser P (2010) Bimetallic Ru Electrocatalysts for the OER and Electrolytic Water Splitting in Acidic Media. Electrochem Solid-State Lett 13:B36
99. Park J, Choi S, Oh A, Jin H, Joo J, Baik H, Lee K (2019) Hemi-core@frame AuCu@IrNi nanocrystals as active and durable bifunctional catalysts for the water splitting reaction in acidic media. Nanoscale Horiz 4:727–734
100. Hartig-Weiss A, Miller M, Beyer H, Schmitt A, Siebel A, Freiberg ATS, Gasteiger HA, El-Sayed HA (2020) Iridium Oxide Catalyst Supported on Antimony-Doped Tin Oxide for High Oxygen Evolution Reaction Activity in Acidic Media. ACS Appl Nano Mater 3:2185–2196
101. Luo J, Tian X, Zeng J, Li Y, Song H, Liao S (2016) Limitations and Improvement Strategies for Early-Transition-Metal Nitrides as Competitive Catalysts toward the Oxygen Reduction Reaction. ACS Catal 6:6165–6174
102. Retuerto M, Pascual L, Calle-Vallejo F, Ferrer P, Gianolio D, Pereira AG, Garcia A, Torrero J, Fernandez-Diaz MT, Bencok P, Pena MA, Fierro JLG, Rojas S (2019) Na-doped ruthenium perovskite electrocatalysts with improved oxygen evolution activity and durability in acidic media. Nat Commun 10:2041
103. Song HJ, Yoon H, Ju B, Kim DW (2020) Highly Efficient Perovskite-Based Electrocatalysts for Water Oxidation in Acidic Environments: A Mini Review. Adv Energy Mater 11:2002428
104. Edgington J, Schweitzer N, Alayoglu S, Seitz LC (2021) Constant Change: Exploring Dynamic Oxygen Evolution Reaction Catalysis and Material Transformations in Strontium Zinc Iridate Perovskite in Acid. J Am Chem Soc 143:9961–9971
105. Chen Y, Li H, Wang J, Du Y, Xi S, Sun Y, Sherburne M, Ager JW, 3rd; Fisher, A. C., Xu, Z. J. (2019) Exceptionally active iridium evolved from a pseudo-cubic perovskite for oxygen evolution in acid. Nat Commun 10:572
106. Chang SH, Danilovic N, Chang KC, Subbaraman R, Paulikas AP, Fong DD, Highland MJ, Baldo PM, Stamenkovic VR, Freeland JW, Eastman JA, Markovic NM (2014) Functional links between stability and reactivity of strontium ruthenate single crystals during oxygen evolution. Nat Commun 5:4191
107. Immerz C, Paidar M, Papakonstantinou G, Bensmann B, Bystron T, Vidakovic-Koch T, Bouzek K, Sundmacher K, Hanke-Rauschenbach R (2018) Effect of the MEA design on the performance of PEMWE single cells with different sizes. J Appl Electrochem 48:701–711
108. Mo J, Kang Z, Yang G, Retterer ST, Cullen DA, Toops TJ, Green JB, Zhang F-Y (2016) Thin liquid/gas diffusion layers for high-efficiency hydrogen production from water splitting. Appl Energy 177:817–822
109. Grigoriev SA, Millet P, Volobuev SA, Fateev VN (2009) Optimization of porous current collectors for PEM water electrolysers. Int J Hydrogen Energy 34:4968–4973
110. Lædre S, Kongstein OE, Oedegaard A, Karoliussen H, Seland F (2017) Materials for Proton Exchange Membrane water electrolyzer bipolar plates. Int J Hydrogen Energy 42:2713–2723
111. Jung H-Y, Huang S-Y, Ganesan P, Popov BN (2009) Performance of gold-coated titanium bipolar plates in unitized regenerative fuel cell operation. J Power Sources 194:972–975
112. Lettenmeier P, Wang R, Abouatallah R, Saruhan B, Freitag O, Gazdzicki P, Morawietz T, Hiesgen R, Gago AS, Friedrich KA (2017) Low-Cost and Durable Bipolar Plates for Proton Exchange Membrane Electrolyzers. Sci Rep 7:44035
113. Feng Q, Yuan XZ, Liu G, Wei B, Zhang Z, Li H, Wang H (2017) A review of proton exchange membrane water electrolysis on degradation mechanisms and mitigation strategies. J Power Sources 366:33–55

Publisher's Note